Vol. 71, Part I, 2001

National Academy of Sciences, India, Allahabad

राष्ट्रीय विज्ञान अकादमी, भारत, इलाहाबाद

Equalized electronegativity and chelation

B.S. SEKHON

Department of Chemistry, Punjab Agricultural University, Ludhiana-141 004, India

Abstract

The concept that a chemical reaction may go in the direction of increased total equalized electronegativity (Xeq) has been explained for substitution reactions involving complexation by monodentate ligands and chelation by polydentate ligands. It is observed that increase in Xeq is even more in case of substitution reactions involving polydentate ligands which leads to products having greater number of chelate rings.

(**Keywords :** electronegativity/chelation/stability of metal chelates)

Introduction

Although the principle of electronegativity equalization[1] has been cited in chemistry literature since 1951 its application [equalized electronegativity (Xeq)] has not been fully exploited except to calculate the partial charges on atoms and groups[2], and to Pearson hard-soft-acid-base reactions[3]. Chelating ligands, the chelate effect and the stability increment resulting from chelation is well known[4]. The chelate effect for a n-dentate chelating ligand refers to the reaction where the chelating ligand replaces the n-unidentate analogous.

M (unidentate)$_n$ + Chelate $\rightleftharpoons$ M (Chelate) + n-unidentate
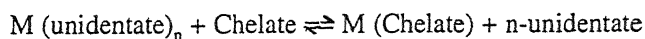
In this work, some applications of Xeq to substitution reactions involving complexation by unidentate ligand and chelation by polydentate ligands are discussed.

Method

Xeq values for various species in substitution reactions were calculated using Bratsch method[5] according to equation

$$Xeq = \frac{N+q}{\sum (v/x)}$$

where $N = \sum v =$ the number of atoms in the species formula, q is the charge of the species and X is the Pauling electronegativity.

Results and Discussion

The following examples (Table 1, reactions 1-13) of the substitution reactions are now examined in terms of total Xeq values of the products and reactants. Reactions 1-13 are substitution reactions of the type

$$M (H_2O)_x^{+m} + L^{-n} = M (H_2O)_{x-1} L^{+(m-n)} + H_2O$$
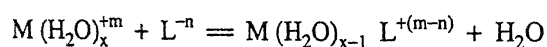
If L were a polydentate ligand then two or more molecules of water would be displaced from the coodination sphere of the complex. It is obvious that Xeq i.e. ($\sum Xeq$ Products $-$ $\sum Xeq$ Reactants) is greater than zero for reactions (1- 13), thereby suggesting that a substitution reaction of above type proceeds in the direction of increase in the total Xeq value of products in comparison to the total Xeq of the reactants. Some results are compiled from literature on stability constants of complexation reactions 1-13 (Table 1). It is observed that increase in Xeq value i.e. ΔXeq is greater for reactions 2, 4 and 6 involving bidentate ligand (en) as compared to ΔXeq for reactions 1, 3 and 5 respectively involving only unidentate ligand. The increase in ΔXeq between nonchelated and chelated species forming reactions is 4.79 (reactions 1 and 2) and 2.31 (reactions 3 and 4; reactions 5 and 6). This increase in ΔXeq may be related to the stability of the chelated species.

It is evident from log β_n values (reactions 4, 7 and 8, Table 1) that stability increase with more substitution of H_2O by en from coordination sphere of the metal ion. These

Table 1 – ΔXeq values and stability data for substitution reactions involving complexation*/chelation. Below each species the number refers to its Xeq value.

Sr. No.	Reaction	Xeq (ΣXeq Products - ΣXeq Reactants)	Stability Constant ($\log \beta_n$)
1.	$Cd(H_2O)_4^{2+} + 4CH_3NH_2 = [Cd(CH_3NH_2)_4]^{2+} + 4H_2O$ 2.78 2.34 2.36 2.50	0.22	$\log \beta_4 = 6.5$ (Ref. 7)
2.	$Cd(H_2O)_4^{2+} + 2\,en = [Cd(en)_2]^{2+} + 4H_2O$ 2.78 2.36 2.51 2.50	5.01	$\log \beta_2 = 10.6$ (Ref. 7)
3	$Ni(H_2O)_6^{2+} + 2NH_3 = [Ni(H_2O)_4(NH_3)_2]^{2+} + 2H_2O$ 2.72 2.36 2.64 2.50	0.20	$\log \beta_2 = 5.0$ (Ref. 8)
4.	$Ni(H_2O)_6^{2+} + en = [Ni(en)(H_2O)_4]^{2+} + 2H_2O$ 2.72 2.36 2.59 2.50	2.51	$\log \beta_1 = 7.5$ (Ref. 8)
5.	$Cu(H_2O)_6^{2+} + 2NH_3 = [Cu(H_2O)_4(NH_3)_2]^{2+} + 2H_2O$ 2.73 2.36 2.65 2.50	0.20	$\log \beta_2 = 7.7$ (Ref. 9)
6	$Cu(H_2O)_6^{2+} + en = [Cu(H_2O)_4\,en]^{2+} + 4H_2O$ 2.73 2.36 2.60 2.50	2.51	$\log \beta_1\;10.6$ (Ref. 9)
7	$Ni(H_2O)_6^{2+} + 2en = [Ni(H_2O)_2(en)_2]^{2+} + 4H_2O$ 2.72 2.36 2.52 2.50	5.08	$\log \beta_2 = 13.50$ (Ref. 10)
8	$Ni(H_2O)_6^{2+} + 3\,en = [Ni(en)_3]^{2+} + 6H_2O$ 2.72 2.36 2.47 2.50	7.67	$\log \beta_3 = 17.6$ (Ref. 10)
9.	$Ni(H_2O)_6^{2+} + Gly = [Ni(H_2O)_4\,Gly]^+ + 2H_2O$ 2.72 2.28 2.61 2.50	2.61	$\log \beta_1 = 6.2$ (Ref. 8)
10.	$Ni(H_2O)_6^{2+} + IMDA^{2-} = [Ni(H_2O)_4(IMDA)] + 3H_2O$ 2.72 2.25 2.54 2.50	5.07	$\log \beta_1 = 8.0$ (Ref. 8)
11.	$Ni(H_2O)^{2+} + NTA^{3-} = [Ni(H_2O)_2(NTA)]^- + 4H_2O$ 2.72 2.24 2.48 2.50	7.52	$\log \beta_1 = 11.3$ (Ref. 8)
12.	$Ni(H_2O)_6^{2+} + dien = [Ni(H_2O)_3(dien)]^{2+} + 3H_2O$ 2.72 2.36 2.54 2.50	4.96	$\log \beta_1 = 10.5$ (Ref. 8)
13.	$Ni(H_2O)_6^{2+} + trien = [Ni(H_2O)_2(trien)]_2+ + 4H_2O$ 2.72 2.36 2.50 2.50	7.42	$\log \beta_1\;13.7$ (Ref. 8)

*Abbreviations : en-$H_2N\,CH_2\,CH_2\,NH_2$; pn – $H_2N(CH_2)_3\,NH_2$; dien – $H_2N\,CH_2\,CH_2\,NH\,CH_2\,CH_2\,NH_2$; trien–$H_2N\,CH_2CH_2\,NHCH_2CH_2\,NH\,CH_2\,CH_2\,NH_2$; $IMDA^{2-}$ – $HN\,(CH_2COO^-)_2$; NTA^{3-} – $N(CH_2COO^-)_3$

observations find support from ΔXeq values which increase on substitution of H_2O by greater number of en.

It is well established that a ligand with greater number of chelate rings forms even the more stable complex[6]. This is obvious from stability data (log β_1 values) for a series of amino-carboxylate ligands $GLY^- < IMDA^{2-} < NTA^{3-}$ (reactions 9, 10 and 11 respectively). Likewise in the amine-ligand series, the stability constants increase as : en < dien < trien which correspond to reactions 4, 12 and 13 respectively. Such stability order is evident from ΔXeq values (Table 1) which also follow the sequence : $GLY^- < IMDA^{2-} < NTA^{3-}$; en < dien < trien. The number of chelate ring formed is one each in gly$^-$ and en, two each in $IMDA^{2-}$ and dien, and three each in NTA^{-3} and trien. It is, therefore, evident from ΔXeq values that more is the number of chelate rings formed by a polydentate ligand, the larger is the increase in ΔXeq in substitution reactions involving chelation.

References

1. Sanderson, R.T. (1951) *Science* **114** : 670.

2. Bratsch, S.G (1984) *J. Chem. Educ.* **61** : 588.

3. Sekhon, B.S. (1996) *Proc. Nat. Acad. Sci. India* **66A** : 217.

4. Cotton, F.A. & Wilkinson, G. (1988) *Advanced Inorganic Chemistry*, 5th Ed., Wiley, New York, pp. 46-48.

5. Bratsch, S.G. (1985) *J. Chem. Educ.* **62** : 101.

6. Martell, A.E. (ed.) (1971) *Coordination Chemistry*, Vol 1, ACS Monograph, Van Nostrand Reinhold Company, New York, pp. 470.

7. Sharpe, A.G. (1992) *Inorganic Chemistry,* 3rd Edn. ELBS, Longman, Group IUK, Ltd., p. 180.

8. Eichhorn, G.L. (ed.) (1973) *Inorganic Biochemistry,* Vol. 1, Chapter 2, Elsevier Scientific Publishing Company, New York, p. 79-82.

9. Shriver, D.F., Atkins, P.W. & Langford, C.H. (1991) *Inorganic Chemistry,* ELBS, Oxford Univ. Press, p. 220.

10. Martel, A.E. & Smith, R.M. (1974-1989) *Critical Stability Constants,* Vol. 1-6, Plenum Press.

Studies on synthesis of some novel bifunctional reactive dyes and their application on various fibres

M.S. PATEL, S.K. PATEL and K.C. PATEL*

Department of Chemistry, South Gujarat University, Surat 395 007, India

* *Author for correspondence.*

Abstract

New synthetic azo reactive dyes have been prepared by coupling diazotised 4,4'-methylene bis-orthoanisidine with various anilino cyanurated coupling component and their dyeing performance as hot brand reactive dyes have been assessed on viscose rayon, silk and wool fibres. These dyes have been found to give a wide range of violet to brown shades with very good depth and levelness on each fibre. These dyes were characterised by elemental analysis, IR and PMR data.

(Keywords : IR/4,4'-methylene-bis ortho anisidine/bis-azo reactive dyes/viscose rayon/ silk/wool).

Introduction

The mono chloro triazinyl reactive system is of major commercial importance in reactive dyeing.[1,2] In recent years a large number of monochloro triazinyl reactive dyes of different types have been synthesised for natural and synthetic fibres[3,4]. The research based on bifunctional reactive dyes has been widely considered due to there higher fixation yield on various fibres[5]. The dyes with two reactive groups give a higher fixation than dies with one reactive group[6,7]. In the present paper, we report the synthesis and dyeing performance of ten hot brand bifunctional reactive dyes.

Materials and Method

All the melting points (m.p.) were determined in open capillaries and are uncorrected. The IR spectra were recorded on Shimadzu Japan DR 8001 (FTIR) spectrophotometer by using Nuzolmull techniques and PMR spectra on a Varian 300 MHz instrument using TMS as internal standard and $CDCl_3$ + DMSO-d_6 as solvent. Fastness tests were assessed by the standard method of testing (BS : 1006 – 1978 and IS : 765 – 197).

Preparation of 4,4'-methylene-bis-ortho-anisidine (A) : Ortho-anisidine (12.3g, 0.1 mol) was dissolved in water (125 ml) and 36.5% hydrochloric acid (25 ml) at 50°C. The reaction mixture was then reacted with 3% aqueous formaldehyde (25 ml) solution at 60°C with stirring for an hour and neutralized with 10% sodium hydroxide, when yellow precipitates were obtained and filtered, washed with hot water, dried and crystallised from acetic acid, Yield 88%, m.p. 100 – 101°C (Found : C, 69.40%; N, 10.60%. $C_{15}H_{18}O_2N_2$ requires : C, 69.76%; N, 10.85%).

Tetrazotization of 4,4'-methylene-bis-ortho-anisidine (B) : 4,4'-Methylene-bis-ortho-anisidine (A) (2.58 g, 0.01 mol) was suspended in H_2O (60 ml). Hydrochloric acid (10 ml) was added dropwise to this well stirred suspension. The mixture was gradually heated upto 70°C, till a clear solution was obtained. The solution was then cooled to 0-5°C in an ice-bath and a solution of $NaNO_2$ (1.2 g) in H_2O (8 ml) previously cooled to 0°C, was then added to it over a period of 5 min. with stirring. The stirring was continued for an additional hour, maintained at the same temperature, with positive test for nitrous acid on starch-iodide paper. After destroying excess of nitrous acid with required amount of a solution of sulphamic acid, a clear tetrazo solution was obtained which was used for subsequent coupling reaction (Reaction 1).

Prepartion of anilino cyanurated coupling components (R) : The coupling components were prepared in two steps (Reaction 2).

(i) Preparation of cyanurated coupling components (R") : A solution of cyanuric chloride (3.70 g, 0.02 mol) in acetone (50 ml) was stirred at a temperature below 5°C for a period of an hour. A neutral solution of coupling components (R') (0.02 mol) in aqueous sodium carbonate solution (10% w/v) was then added to it in small lots in about an hour. The pH of the solution was maintained at 7 by simultaneous addition of sodium carbonate solution (1% w/v). The temperature was maintained below 5°C for further 4 h when a clear solution was obtained. The cyanurated solution (R") thus formed was used subsequently.

(ii) Formation of anilino cyanurated coupling component (R) : The cyanurated coupling component (R") was heated upto 40- 50°C for half an hour. Then aniline (1.86% g. 0.02 mol) was added to it dropwise at the same temperature, during a period of 30 min. maintaining the pH at 7 by simultaneous addition of sodium bicarbonate solution (1% w/v). After the addtion was completed, stirring was continued for further 3 h. The anilino cyanurated coupling component (R) thus obtained was used for further coupling reaction.

Formation of Dyes (D_1 to D_{10}) : To an ice-cold and well stirred solution of anilino cyanurated coupling component (R), a freshly prepared solution of tetrazo soluton (B) was added dropwise over a period of 10–15 min. The pH was maintained at 7.5–8.5 during the addition

SOME NOVEL BIFUNCTIONAL REACTIVE DYES
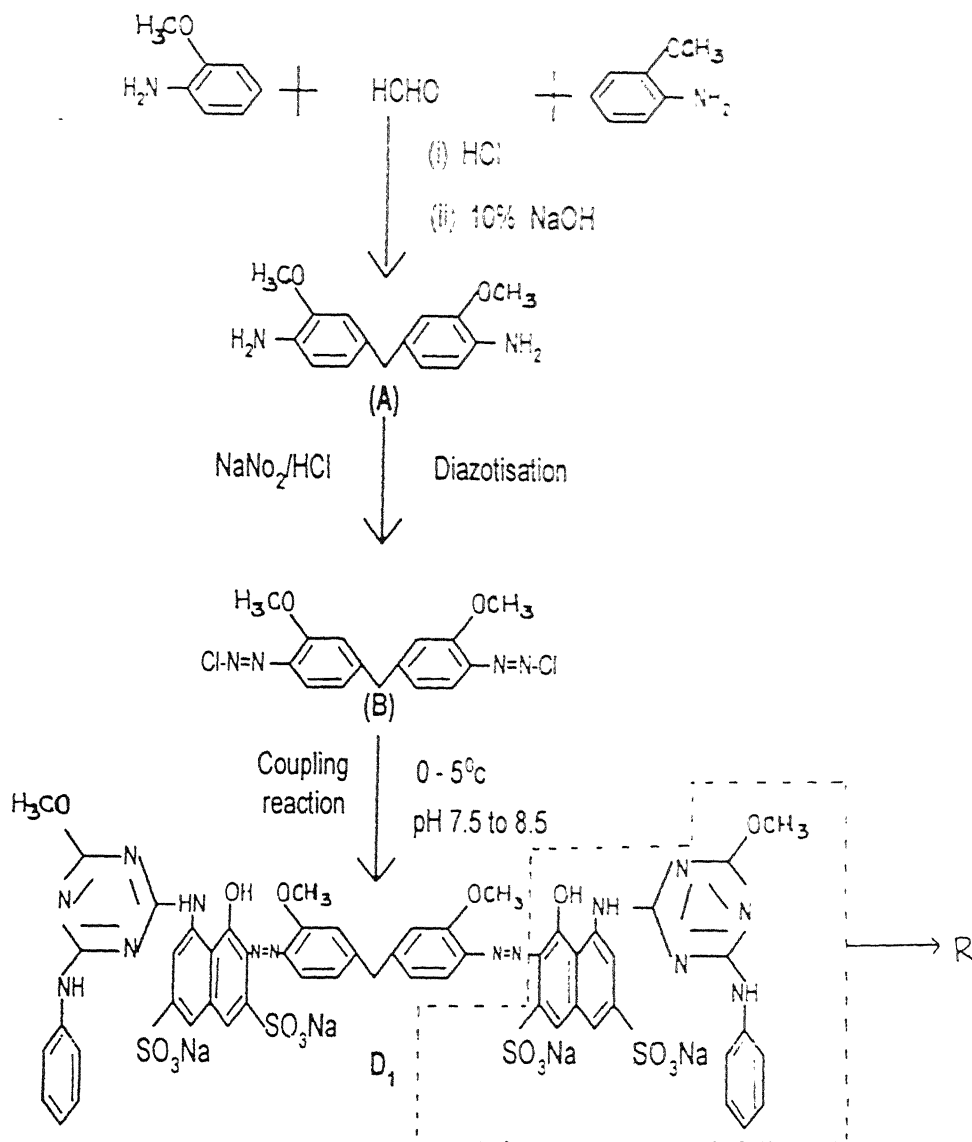
Where, R = Various anilino cyanurated coupling components
for the formation of D₁ to D₁₀ (Table - 1).

Reaction 1

(R")
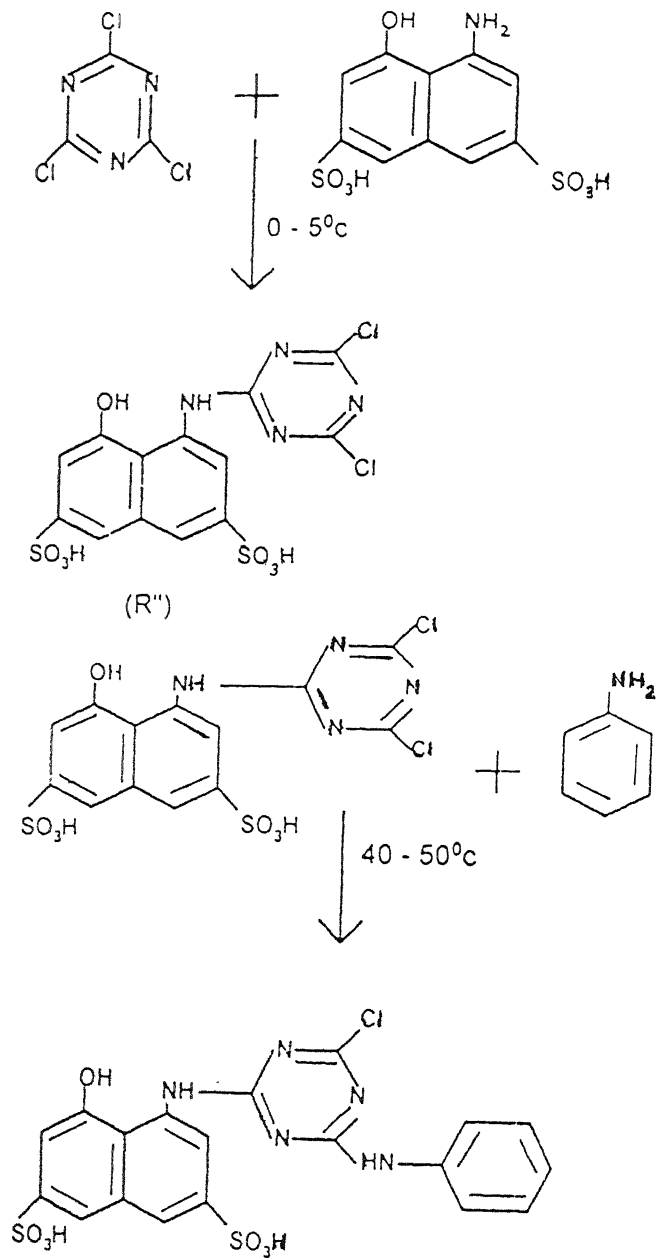
Reaction 2

Table 1 – Yield, λ_{max}, m.p., Rf and elemental analysis of the prepared dyes

Dye No.	Anilino cyanurated component coupling	Molecular formula	Mol. Wt.	Yield (%)	M.P. (°C)	λ_{max} a	Rf value b	Found (Calculated)%			
								C	H	N	S
D_1	H-acid	$C_{53}H_{36}O_{16}N_{14}Cl_2S_4Na_4$	1367	82	355	510	0.45	46.30 (46.52)	2.60 (2.63)	14.30 (14.33)	9.32 (9.36)
D_2	K-acid	$C_{53}H_{36}O_{16}N_{14}Cl_2S_4Na_4$	1367	80	382	440	0.39	46.40 (46.52)	2.58 (2.63)	14.28 (14.33)	9.30 (9.36)
D_3	J-acid	$C_{53}H_{38}O_{10}N_{14}Cl_2S_2Na_2$	1187	84	357	420	0.42	47.00 (47.04)	3.15 (3.20)	16.45 (16.51)	5.35 (5.39)
D_4	Tobias acid	$C_{53}H_{38}O_8N_{14}Cl_2S_2Na_2$	1155	86	343	455	0.40	55.00 (55.06)	3.25 (3.29)	16.90 (16.96)	5.49 (5.54)
D_5	Gamma acid	$C_{53}H_{38}O_{10}N_{14}Cl_2S_2Na_2$	1187	84	353	430	0.41	46.90 (47.04)	3.12 (3.20)	16.48 (16.51)	5.35 (5.39)
D_6	N-methyl J-acid	$C_{55}H_{42}O_{10}N_{14}Cl_2S_2Na_2$	1237	72	348	445	0.44	53.10 (53.35)	3.34 (3.39)	15.80 (15.84)	5.13 (5.17)
D_7	N-phenyl J-acid	$C_{65}H_{46}O_{10}N_{14}Cl_2S_2Na_2$	1339	74	378	515	0.41	58.15 (58.25)	3.40 (3.43)	14.58 (14.63)	4.70 (4.77)
D_8	Sulpho tobias acid	$C_{53}H_{36}O_{14}N_{14}Cl_2S_4Na_4$	1355	75	362	485	0.38	46.85 (46.93)	2.60 (2.65)	14.42 (14.46)	9.41 (9.44)
D_9	Schaffer acid	$C_{53}H_{36}O_{10}N_{12}Cl_2S_2Na_2$	1157	78	355	495	0.47	54.90 (54.96)	3.09 (3.11)	14.47 (14.52)	5.50 (5.53)
D_{10}	Chicago acid	$C_{53}H_{36}O_{16}N_{14}Cl_2S_4Na_4$	1367	73	345	465	0.46	46.40 (46.52)	2.61 (2.63)	14.30 (14.33)	9.30 (9.36)

a) Determined in DMF at 20°C in 2×10^{-3} M concentration

b) Determined by TLC using benzyl chloride - DMF - Water (30 20 20) mixture as solvent or silica Gel - G as at sorbent.

Table 2 - Shade, percentage exhaustion and fastness properties of hot brand reactive dyes on viscose rayon, silk and wool.

Dye No	Shade on dyed Fibre	% Exhaustion			Light fastness (a)			Wash fastness (b)			Rubbing fastness (c)					
											Wet			Dry		
		V	S	W	V	S	W	V	S	W	V	S	W	V	S	W
D_1	Violet	72.25	57.00	53.50	4-5	2	3-4	4	3	3	5	4	4	5	4-5	4
D_2	Yellow	76.00	55.00	55.00	4-5	2	4	3-4	3	3	5	4	3-4	5	4	4
D_3	Maroon	73.75	60.25	48.75	4-5	2	3-4	4	3-4	3-4	5	4	4	5	4	4-5
D_4	Brown	72.00	60.50	51.50	5	4·5	4	4	3-4	4	5	4	4	5	4	4
D_5	Dark brown	76.50	59.25	53.00	5	2	4	4	4	3-4	4	4-5	3	4	4	3
D_6	Reddish brown	73.00	59.50	51.75	4	2	4	3-4	3-4	3	4-5	4	4	4	4	4
D_7	Light yellow	72.50	60.75	52.50	3-4	3	3	3	3	3	4	3-4	4	4	3	3
D_8	Yellowish brown	73.10	58.85	51.95	3-4	3	3	3	2-3	3	4	3-4	3-4	4	3	3
D_9	Light brown	74.25	55.25	53.75	4	3-4	3	3-4	3	3	4	4	4	4	3	3
D_{10}	Reddish brown	75.20	60.10	54.20	3	2·3	3	3	2	3	3	3	3	3	3	2-3

(a-b-c) Determined using usual procedure
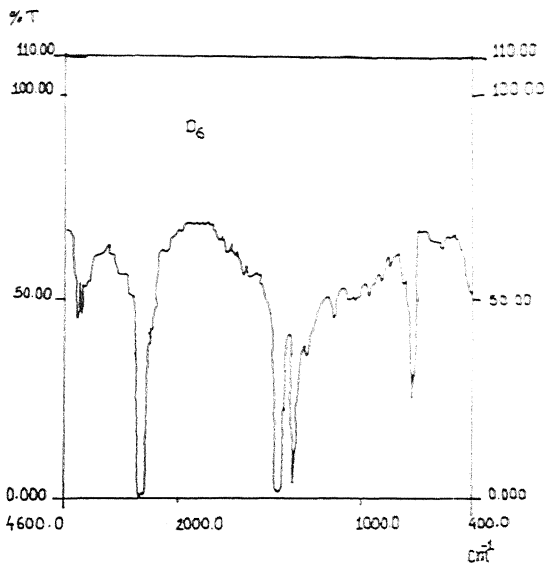
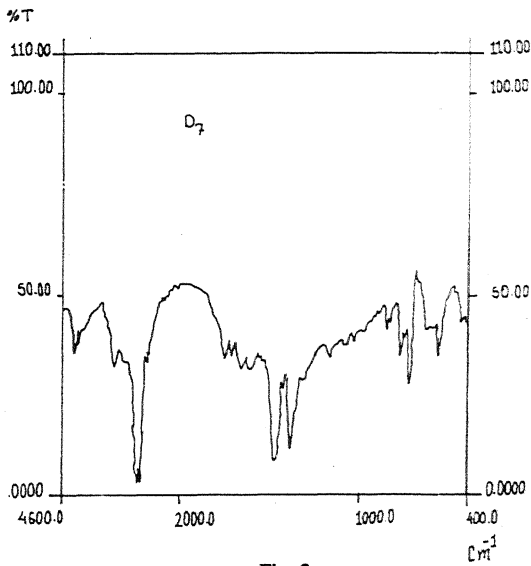V= Viscos rayon, S = Silk, W = Wool

Fig. 1

Fig. 2

and stirring was continued for 4 h, maintaining the temperature below 5°C. Sodium chloride (12 g) was then added and the mixture was stirred for an hour. The solid dye separated out was filtered, washed with minimum amount of acetone and dried at room temperature (Table 1).

Results and Discussion

The dyes were violet to brown colour and obtained in excellent yield (72 to 86%). The purify of all dyes has been checked by thin-layer chromatography[8]. The yield (%), m.p., λmax, *Rf* value and elemental analysis data of dyes are reported in Table 1. The shade and the fastness properties are reported in Table 2.

IR Spectra : The IR spectra of dyes D_1 to D_{10} showed characteristic band at 2940-2925 ($-CH_2-$)[9], 1730-1725 (C=O), 775-760 (S-triazine), 725-715 (C-Cl), 1480-1470 (-NH), 1385-1380 (-N=N-), 1090-1075 (S=O), 3450-3400 cm^{-1} due to O-H stretching vibrations. The IR spectra of some hot brand reactive dyes are shown in Fig.1, 2.

PMR Spectra : In general the dyes show a singlet peak at δ 4.80–4.05 (2H, $-CH_2-$), 5.78–5.08 (2H, Ar-OH), 4.80–3.78 (2H, -NH-Ar) and around 7.5–8.7 (aromatic protons)

Dyeing : The dyes varied in hue from light to dark shade of violet to brown colour depending on the nature of substituent present in the coupling component. The result shows that the presence of the e⁻ donating groups increase the bathochromic effect. However, the light fastness appears to be good to excellent because of higher molecular weight. The overall dyeing properties appear to be good to excellent.

References

1. Siegel, E. (1972) *"The Chemistry of Synthetic Dyes"*, ed. K. Venkatraman, Academic Press, New York 6 : 1.

2. Stead, C.V. (1982) *Dyes and Pigments* 3 : 161.

3. Naik, V.R. & Desai, K.R. (1992) *Proc. Nat. Acad. Sci. India* 62(A) : 373. ·

4. Mistry, N.V., Desai, V.R. & Desai, K.R. (1992) *Nat. Acad. Sci. Letters* 15(7) : 207.

5. Cassela, C.A. (1959) G.P. : 1794297.

6. Bredereck, K. & Schumacher, C. (1993) *Dyes and Pigments* 21 : 23.

7. Matsi Maski, Ulrich Meyer & Zollinger, H. (1988) *J. Soc. Dyers Colour* 104 : 425.

8. Fried-Bernard & Sherma Josep (1982) *"Thin-Layer Chromatography Techniques and Application"*, Marcel Dekker, Inc., New York and Basel.

9. Colthup, N.B., Daly, L.H. & Stephen, Wibeley, E. (1975) *"Introduction to Infrared and Raman Spectroscopy"*, Academic Press, New York, San Francisco, London.

Study of metal drug equilibria in solution

PURUSHOTTAM B. CHAKRAWARTI*, MUKTA CHAKRAWARTI and PRAMILA MAINI

Chemistry Department, Motilal Vigyan Mahavidyalaya, Bhopal-462 002, India

* Address for correspondence., A-252, Shahpura, Bhopal-426 016, India.

Abstract

The interaction of Mg(II), Mn(II) and Cd(II) ions with cephalexin, a wide spectrum antibiotic drug of cephalosporin group, in presence of biologically important ligand α-alanine has been investigated by potentiometric studies. The proton dissociation constant of cephalexin, stability constants of the binary complexes of 1:1 and 1:2, and ternary complexes of 1:1:1 molar ratios of the metal ion to ligand have been reported at 25° and 35°C and 0.1M (NaCl$_4$) ionic strength. The order of stability constants follows as Cd(II) > Mg(II) > Mn(II). Thermodynamic parameters (ΔG, ΔH and ΔS) calculated at 35°C and 0.1M ionic strength indicate that the drug-metal ions and alanine interactions are enthalpy characterised.

(**Keywords** : metal-drug equilibria/stability constant/mixed-ligand complexes/Cd(II)/Mg(II) complexes/cephalexin complexes)

Introduction

It is well known that ternary complexes play an important role in biological processes in which enzymes are known to be activated by metal ions[1]. Ternary complexes have also been implicated in the storage and transport of active substances through biological membranes. These phenomena depend upon the formation of higher order complexes and the nature of involed metal ions with antibiotic drugs. In the presence of amino acid the enzyme may yield useful information for elucidating the molecular mechanism of drug action. In this paper, the results of the study of metal-cephalexin-alanine equilibria in solution are reported.

Cephalexin is one of the most important semi-synthetic cephalosporins. Cephalexin has benzalamine ($C_6H_5CH.NH_2-$) and hydrogen (H) groups present at R_1 and R_2 respectively in 7-amino-cephalosporanic acid molecule.

Materials and Method

All the chemicals used were of A.R. or S.M grade. Cephalexin sample was obtained from Lupin Pharma Ltd., Mandideep, Bhopal (India).

(I) 7-Aminocephalosporanic acid   (II) Cephalexin
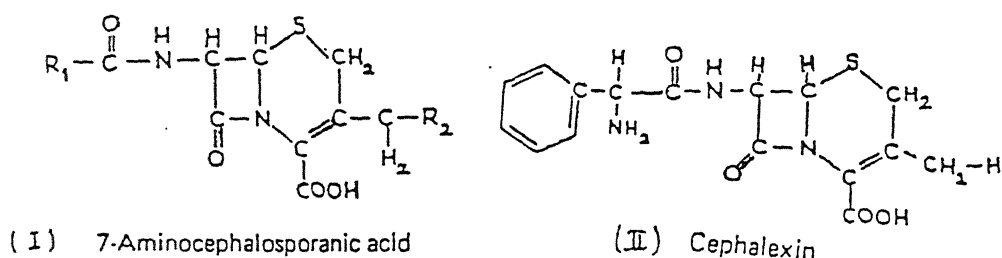
The preparation and standardisation of the metal ions and the ligand solutions, and the experimental details are the same as reported earlier[2].

Stoichiometry of the complexes formed was ascertained by conductometric titrations. The Calvin-Bjerrum's pH-titration technique as modified by Irving and Rossotti[3-5] was applied to determine various formation constants at 25° and 35°C and 0.1M ($NaClO_4$) ionic strength. For pH-titrations the following thermostated mixtures were titrated with the carbonate-free 0.1M NaOH solution:

(a) 10 ml 0.04M $HClO_4$ + 1.0M $NaClO_4$

(b) Mixture (a) + 5 ml 0.004M cephalexin

(c) Mixture (a) + 5 ml 0.004M alanine

(d) Mixture (b) + 10 ml 0.002M metal

(e) Mixture (c) + 10 ml 0.002M metal

(f) Mixture (b) + 5 ml 0.004M alanine

(g) Mixture (f) + 10 ml 0.002M metal
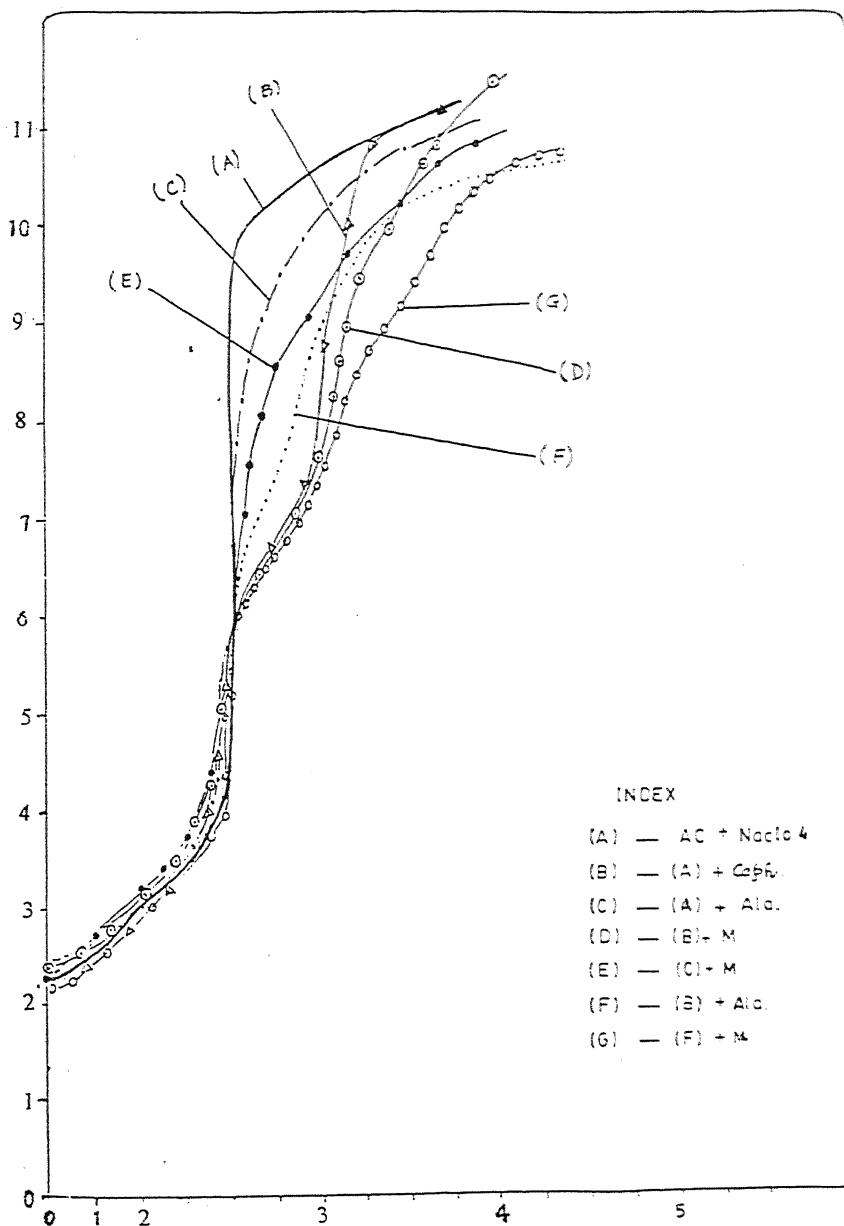
Fig. 1 – pH titration curves. Ceph-Ala system.

Table 1 – Stability constants and thermodynamic parameters $\mu = 0.1M$ (NaCO$_4$); Temp. = 25°C (a) and 35°C (b) x = half integral, y = Least square method.

Constants	H	Mg	Mn	Cd
$\log K_1^H$	(a) 3.50^y			
	(b) 3.25^y			
$\log K_2^H$	(a) 8.75^y			
	(b) 7.50^y			
$\log K_{ML}^M$	(a)	5.35^x	4.47^x	5.77^x
		5.27^y	4.47^y	5.60^y
	(b)	5.00^x	4.25^x	5.22^x
		5.00^y	4.21^y	5.20^y
$\log K_{ML_2}^{ML}$	(a)	3.45^x	3.37^x	3.55^x
		3.40^y	3.32^y	3.55^y
	(b)	3.32^x	3.15^x	3.45^x
		3.29^y	3.12^y	3.42^y
$\log\beta_2$	(a)	8.70^x	7.84^x	9.32^x
		8.67^y	7.79^y	9.15^y
	(b)	8.32^x	7.40^x	8.67^x
		8.29^y	7.33^y	8.62^y
$\log K_{MLA}^{ML}$	(a)	4.93^x	4.38^x	5.28^x
		4.96^y	4.36^y	5.25^y
	(b)	4.58^x	3.95^x	4.77^x
		4.55^y	3.92^y	4.78^y
$\Delta\log K$ $\log\left(K_{MLA}^{ML} - K_{ML}^M\right)$	(b)	-0.45^y	-0.29^y	-0.42^y
$-\Delta G$ (Kcal/mole)		6.46^y	5.56^y	6.78^y
$-\Delta H$ (— do —)		17.31^y	18.57^y	19.84^y
$-\Delta S$ (cal/deg/mole)		$+35.22^y$	42.24^y	42.40^y

The ionic strength of the above solutions was maintained to 0.1M by adding required quantity of 1.0M $NaClO_4$ solution and the total volume of the solution to be titrated was made 50 ml by the addition of required volume of distilled water.

The values of $\bar{n}A$, $\bar{n}$ and pL were claculated by using the Irving- Rosotti equations[3-5] Proton-ligand stability constant, K_n^H for cephalexin was obtained by using (i) the half integral (from the plot of $\bar{n}A$ vs pH) and (ii) the pointwise calculation methods; while the values of log K_{ML}^M $K_{ML_2}^{ML}$ and K_{MLA}^{ML} for the metal complexes were recorded from the formation curves. The refined values obtained from the least square method are given in Table 1.

Thermodynamic parameters computed for the complexation reactions studied in this investigation are free energy (ΔG), enthalpy (ΔH) and entropy (ΔS) changes. These have been calculated using the Vant Hoff isotherm, Vant Hoff equation and the Gibbs Helmhotz equatons respectively at 35°C and at ionic strength of 0.1M with $NaClO_4$.

Results and Discussion

Conductometric studies of the metal drug and metal alanine equilibria in solution utilising Nair and Pande's mono-variation method[6] indicated the formation of two complexes in this system, with the molar ratio (metal : drug or metal : alanine) 1:1 and 1:2 respectively.

$$M + L = ML$$

$$ML + L = ML_2$$
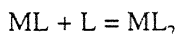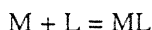
where, M = the divalent metal ion, and L = cephalexin or alanine molecule or its ion.

Charges on the species have been omitted for simplicity. Addition of third molecule of the ligand did not take place probably due to steric hindrance of the bulky molecules in accordance with the earlier reported results with penicillin and cephalosporin groups of drugs[7-12].

The pH titraton curves in the cases of cephalexin and alanine lie before the acid curve (Fig. 1), indicating that in acidic solutions each molecule of the ligand is in association with one equivalent of proton. This proton should be attached with the lone pair of electrons present on the nitrogen of the β- lactam thiozolidine ring in case of cephalexin and on the nitrogen of amino group in case of alanine as indicated in the earlier studies[2,7] this corresponds with the two successive steps of deprotonation of the protonated ligands:

$$HLH^+ = H^+L^- + H^+ \qquad (1)$$

$$H^+L^- = L^- + H^+ \qquad (2)$$

Eqn. (1) corresponds with the ionisation of the carboxyl group of the ligands, while equation (2) denotes deprotonation of the proton attached to the nitrogen atom. The former takes place in the pH range 3.5 to 5 while the later is observed between pH 6.5 to 10.

Earlier reports[7-12] also indicate similar steps of deprotonation for the protonated species of penicillin and cephalosporin drugs and alanine.

Representative set of experimental titration curves obtained according to the sequence for different M(II) : drug : alanine systems studied reveals that below pH 6.4 formation of different M(II) : drug (cephalexin) binary complexes takes place. Thus the drug species, L^- may coordinate with M(II) ions as a (N,O) donor ligand using nitrogen of OCN group and oxygen of carboxyl group. This is clear from the appeared divergence of each of the 1:1 binary M(II)-drug titration curve from that of the corresponding free drug curve. Generally such complexes are stable upto pH 5-8 in case of different metal ions. Beyond these pH values, hydrolysis of the complexes leads to the formation of hydroxocomplex species.

Careful examination of titration curves of the ternary complex reveals that the 1:1:1 mixed ligand complexes are formed at pH values higher than those corresponding to the formation of the binary complexes of the drug (Cephalxin). This behaviour indicates that the binary complex ML is first formed and it coordinates with alanine(A) as secondary ligand to yield the mixed ligand complex MLA in a stepwise manner, similar to the formation of 1:2 binary complex. Further the mixed ligand curve(F) and ML(binary) curves are overlapped at relatively low pH values indicating that the amino acid does not bind with the metal ion in this range. At high pH the divergence of the two curves takes place. As the proton attached to the nitrogen is not removed below pH 5, hence the stepwise complexation equilibria can be represented as follows :

$$M^{++} + H^+L^- = (ML) + H^+ \qquad (3)$$

$$(ML)^+ + HAH^+ = (MLA) + 2H^+ \qquad (4)$$

where H^+L^- = protonated cephalexin ion, and HAH^+ = protonated alanine molecule.

(a) Proton Ligand Stability Constants : The proton ligand stability constants of the drugs cephalexin have been calculated at 25°C and 35°C and 0.1M (NaClO$_4$) utilising the Irving Rossotti pH titration technique.[3,4]

With the increase in temperature, the values of log K_n^H decreases showing an exothermic change i.e., with increasing temperature ligand show dissociation of the species.

(b) Metal Ligand Formation Constants : The stability constants of 1:1 and 1:2 binary and 1:1:1 ternary complexes were calculated at two temperatures 25° and 35°C and at 0.1M ionic concentration, utilising Irving- Rossotti method and its modification for ternary systems.[3-5]

The values obtained for the binary and ternary complexes are reported in Table 1.

The ternary complexes are characterised by values of log log K_{MLA}^{ML} and Δlog K (Table 1).

The results reveal that in general with the increase in the temperature log K_{ML}^M and log K_{MLA}^{ML} values decrease, indicating exothermic nature of complexation reactions,

$$M + L = ML \tag{3}$$

$$ML + A = MLA \tag{4}$$

A comparision of the stability constants (Table 1) of the binary and ternary complexes of the metal ions with the drug (cephalexin) and alanine gives interesting results. It may be noted that the ternary complexes, MLA, are comparatively more stable than the corresponding 1:2 binary complexes of the drugs. However, the ternary complexes in both the systems are characterised by low stability compared to the corresponding M(II) – drug binary complexes, i.e. $K_{ML}^M > K_{MLA}^{ML}$. Due to statistical, steric and electrostatic considerations the stability constants for the stepwise formation of 1:1:1 ternary (MLA) complex is expected to be smaller than the corresponding binary system and the values of Δlog K $\left(= \log K_{MLA}^{ML} - \log K_{ML}^M \right)$ should be negative[13] as obtained in the present investigation.

According to Sigel a positive/or a value that is less negative than – 0.6 for the stability qualifying factor, Δlog$K$, suggests favoured formation of ternary complex[14]. The Δlog$K$ values obtained in the present study are in general less negative indicating greater stabilization of ternary complexes as compared to the 1:2 binary (ML$_2$) complexes of the drugs (Table 1).

The order with reference to metal ions is, Mn(II) < Mg(II) < Cd(II).

(c) Thermodynamic Parameters : The value of changes in free energy (ΔG), enthalpy (ΔH) and entropy (ΔS) accompanying the formation of the binary and ternary complexes, using the standard equations[15] are reported in Table 1.

The negative values of ΔG show that the driving tendency of the complexation reaction is from left to right and the reaction tends to proceed spontaneously.

References

1. Cortyell, C.C. (1954) *"Special Problem s in the Formation of Metal Complexes in Chemical Specificity in Biological Interactions"*, Ed. R.N. Gurd, Acazd. Press, New York, pp. 90-160.

2. Chakrawarti, P.B., Shrivastava, B. & Vijayvargiya, B.L. (1994) *Proc. Nat. Acad. Sci. India* **64A** : 340.

3. Irving, H. & Rossotti, H.S. (1953) *J. Chem. Soc.* 3397.

4. Irving, H. & Rossotti, H.S. (1954) *J. Chem. Soc.* 2904.

5. Chidambaram, M.V. & Bhattacharya, P.K. (1970) *J. Inorg. Nucl. Chem.* **39** : 2471.

6. Nair, M.R. & Pande, C.S. (1948) *Proc. Indian Acad. Sci.* **27A** : 293.

7. Chakrawarti, P.B., Shrivastava, B. & Vijayavargiya, B.L. (1993) *J. Indian Chem. Soc.* **70** : 160.

8. Chakrawarti, P.B., Tiwari, A. & Sharma, H.N. (1980) *J. Indian Chem. Soc.* **57** : 134.

9. Chakrawarti, P.B., Tiwari, A. & Sharma, H.N (1980) *Indian J. Chem.* **19A** : 83.

10. Mukherjee, G.N. & Ghosh, T.K. (1994) *J. Indian Chem. Soc.* **71** : 249.

11. Mukherjee, G.N. & Ghosh, T.K. (1997) *J. Indian Chem. Soc.* **74** : 539.

12. Mukherjee, G.N. & Ghosh, T.K. (1995) *J. Indian Chem. Soc.* **57** : 827.

13. Mohan, M.S., Bencroft, D. & Abott, F.H. (1979) *Inorg. Chem.* **18** :. 344.

14. Sigel, H. (1975) *Angrew Chem. Int. ED Emgl.* **14** : 394.

15. Kettle, S.F.A. (1973) *Coordination Compounds*, Nelson (EIBS) London.

Thermo-elastic stress distribution in three layered system

ASHOKE DAS and BIMALENDU DAS*

Balurghat High School, D/Dinajpur

Department of Mathematics, North Bengal University, Siliguri 734 430, India

Abstract

This paper is concerned with the determination of thermal stresses in different layers of a three-layered system when the temperature is applied on the surface $z = 0$. This is axisymmetric, elasto-static problem. Transform method has been applied for the solution and numerical values are obtained for resultant stress.

(Keywords : layered problem/axisymmetric/elasto-static/Hane-transform/heat flux/linear temperature distribution).

Introduction

This is an axisymmetric, statical three-layered problem of thermo-elasticity. This paper investigates thermal stresses distributed over three-layered media due to flux of heat applied on a surface $z = 0$ of the upper most layer. Layered problems have been solved by Burmister[1], Nowacki[2] and double layered problem by Paria[3] due to application of concentrated force on the upper face of the layer. Transform technique has been taken for solution. Heat flux is taken to be linear. Experimental result of elastic constants are taken from international critical table[4].

Statement of the Problem

Materials under consideration occupy the lower half of the plane $z = 0$ and the axis of z being taken positive when drawn into the material. Physical quantities involved here all are symmetrical about the z axis. Lower boundaries of the first and second layeres are given by the plane $z = h_1$ and $z = h_2$ and the underlying mass extended to infinity. Interfaces are supposed to be perfectly rough so that stresses and displacement are continuous across it.

Method of Solutions of the Thermo-Elastic Problem

Physical quantities involved in the problem are all symmetric about z-axis, so four non-zero components σ_r, σ_0, σ_z, τ_{zr} and two non-zero displacement components u_r, u_z are retained in terms of stress function Φ satisfying the differential equation[5]

$$\nabla^2 \nabla^2 \phi = \left(\frac{\partial^2}{\partial r^2} + \frac{1}{r}\frac{\partial}{\partial r} + \frac{\partial^2}{\partial z^2} \right)^2 \Phi = 0 \tag{1}$$

Here, stress function Φ due to Hänkel transform[6] will take the form G, defined as

$$G(\xi z) = \int_0^\infty r\,\Phi\,J_0(\xi r)\,dr, \quad (\xi > 0,\ Z > 0) \tag{2}$$

whose inverse is given by

$$\Phi = \int_0^\infty \xi\, G(\xi, Z)\, J_0(\xi r)\, d\xi \tag{3}$$

Let the solution of (1) be given by

$$G(\xi, z) = (A + Bz)\,(2\sin h\,\xi z + e^{-\xi z}) + (C + Dz)\,(2\cosh \xi z - e^{\xi z}) \tag{4}$$

where A, B, C, D are functons of ξ to be determined from the suitable boundary conditions.

To determine the streses, the potential of thermo-elastic displacement ψ, related to the equations,

$$\left. \begin{array}{l} \dfrac{\partial \psi}{\partial r} = (u_r)_T \\[2mm] \dfrac{\partial \psi}{\partial z} = (u_z)_T \end{array} \right\} \tag{5}$$

is considered in the steady state of temperature field given by

$$\nabla^2 T = 0 \tag{6}$$

Since different layers have different thermal properties, different potential displacement functions are chosen. From the stress- strain relations of thermo-elasticity and the equation of equilibrium[3], we have

$$\nabla^2 \psi_i = \beta_i T, \tag{7}$$

$$\beta = \frac{1 + \sigma_i}{1 - \sigma_i} \alpha_i, \quad i = 1, 2, 3$$

where σ_i are Poisson's ratios and α_i the coefficient of linear thermal expansions.

Applying Hankel transform on (6) and (7) we obtain.

$$\left(\frac{d^2}{dz^2} - \xi^2 \right) M(\xi, z) = 0 \tag{8}$$

and

$$\left(\frac{d^2}{dz^2} - \xi^2 \right) L_i(\xi, z) = \beta_i M(\xi, z) \tag{9}$$

where

$$M(\xi, z) = \int_0^\infty r \, T \, J_0(\xi r) \, dr \tag{10}$$

and

$$L_i(\xi, z) = \int_0^\infty r \, \psi_i \, J_0(\xi r) \, dr \tag{11}$$

Let the solution of (11) be

$$L_i(\xi, z) = -\frac{\beta_i}{2\xi^2} A_0 (1 + z \xi) e^{-\xi z} \tag{12}$$

Then the solution of (10) is

$$M(\xi, z) = A_0 e^{-\xi z} \tag{13}$$

where A_0 is a function of ξ.

Applying (12) we have, by using the eqn. (20-22)[3]

$$\int_0^\infty r(\sigma_z)_{T_i} J_0(\xi r) dr = -\mu_i \beta_i (1 + z\xi) A_0 e^{-\xi z} \tag{14}$$

$$\int_0^\infty r(\tau_{zr})_{T_i} J_1(\xi r) dr = -\mu_i \beta_i (z\xi) A_0 e^{-\xi z} \tag{15}$$

$$\int_0^\infty r(u_r)_{T_i} J_1(\xi r) dr = \frac{1}{2\xi} \beta_i (1 + z\xi) A_0 e^{-\xi z} \tag{16}$$

$$\int_0^\infty r(u_r)_{T_i} J_0(\xi r) dr = \frac{1}{2} \beta_i z A_0 e^{-\xi z} \tag{17}$$

Taking solution of (1) for different layers as :

For the upper layer

$$G_1(\xi, z) = (A_1 + B_1 z)(2\sinh \xi z + e^{-\xi z}) + (C_1 + D_1 z)(2\cosh \xi z - e^{\xi z}) \tag{18}$$

For the middle layer

$$G_2(\xi, z) = (A_2 + B_2 z)(2\sinh \xi z + e^{-\xi z}) + (C_2 + D_2 z)(2\cosh \xi z - e^{\xi z}) \tag{19}$$

For the underlying mass

$$G_3(\xi, z) = (A_3 + B_3 z) e^{-\xi z} \qquad \xi > 0, z \geq h_2 \tag{20}$$

It is to be noted that stresses and displacements in the underlying mass vanish as $z \to \infty$. So the components of stress and displacement for the upper and middle layers are obtained by using the eqn. $(63-66)^5$ when $j=1, 2$ are

$$\int_0^\infty r\,(\sigma_z)_j\,J_0\,(\xi r)\,dr = (1 - 2\sigma_j)\,\xi^2\,B_j\,(2\sinh\,\xi z + e^{-\xi z}) + (1 - 2\sigma_j)\,\xi^2\,D_j\,(2\cosh\,\xi z - x^{\xi z})$$

$$+ \xi^3\,(A_j + B_j\,z)\,(e^{-\xi z} - 2\cosh\,\xi z) + \xi^3\,(C_j + D_j\,z)\,(e^{\xi z} - 2\sinh\,\xi z) \qquad (21)$$

$$\int_0^\infty r\,(\tau_{zr})_j\,J_1\,(\xi r)\,dr = 2\sigma_j\,\xi^2\,B_j\,(2\cosh\,\xi z - e^{-\xi z}) + 2\sigma_j\,\xi^2\,D_j\,(2\sinh\,\xi z - e^{\xi z})$$

$$+ \xi^3\,(A_j + B_j\,z)\,(e^{-\xi z} + 2\sin h\,\xi z) + \xi^3\,(C_j + D_j\,z)\,(2\cosh\,\xi z - e^{\xi z}) \qquad (22)$$

$$\int_0^\infty r\,(u_z)_j\,J_1\,(\xi r)\,dr = \frac{1 + \sigma_j}{E_j}\,\xi\Big[B_j\,(e^{-\xi z} + 2\sinh\,\xi\,z) + D_j\,(2\cos\,\xi z - e^{\xi z})$$

$$+ \xi\,(A_j + B_j\,z)\,(2\cosh\,\xi z - e^{\xi z}) + \xi\,(C_j + D_j\,z)\,(2\sinh\,\xi z - e^{\xi z})\Big] \qquad (23)$$

$$\int_0^\infty r\,(u_z)_j J_0\,(\xi r)\,dr = \frac{1 + \sigma_j}{E_j}\,\xi\Big[2(1 - 2\sigma_j)\,B_j\,(2\cosh\xi z - e^{-\xi z}) + 2\,(1 - 2\sigma_j)\,D_j\,(2\sinh\xi z - e^{\xi z})$$

$$- \xi\,(A_j + B_j z)\,(2\sinh\,\xi z + e^{-\xi z}) - \xi\,(C_j + D_j\,z)\,(2\cosh\xi z - e^{\xi z})\Big] \qquad (24)$$

For the underlying mass

$$\int_0^\infty r\,(\sigma_z)_3\,J_0\,(\xi r)\,dr = \xi^3\Big[A_3 + B_3\,z + \frac{B_3}{\xi}\,(1 - 2\sigma_3)\Big]e^{-\xi z} \qquad (25)$$

$$\int_0^\infty r\,(\tau_{zr})_3\,J_1\,(\xi r)\,dr = \xi^3\Big[A_3 + B_3\,z - \frac{2\sigma_3}{\xi}\,B_3\Big]e^{-\xi z} \qquad (26)$$

$$\int_0^\infty r\,(u_r)_3\,J_1\,(\xi r)\,dr \;=\; \frac{1+\sigma_3}{E_3}\left[\frac{B_3}{\xi}\;-\;A_3\;-\;B_3 z\right]e^{-\xi z} \tag{27}$$

$$\int_0^\infty r\,(u_z)_3\,J_0\,(\xi r)\,dr \;=\; \frac{1+\sigma_3}{E_3}\,\xi^3\left[A_3\;+\;B_3\,z\;+\;\frac{2B_3}{\xi}\,(1-2\sigma_3)\right]e^{-\xi z} \tag{28}$$

Boundary condition :

In order to nullify the stresses on the boundaries the following conditions are to be satisfied:

At $z = 0$

$$\left.\begin{aligned}
-\,(u_r)_{T_1} &= (u_r)_1\\
-\,(u_z)_{T_1} &= (u_z)_1\\
-\,(\sigma_z)_{T_1} &= (\sigma_z)_1\\
-\,(\tau_{zr})_{T_1} &= (\tau_{zr})_1
\end{aligned}\right\} \tag{29}$$

At $z = h_1$

$$\left.\begin{aligned}
-\,(u_r)_{T_2} &= (u_r)_2\\
-\,(u_z)_{T_2} &= (u_z)_2\\
-\,(\sigma_z)_{T_2} &= (\sigma_z)_2\\
-\,(\tau_{zr})_{T_2} &= (\tau_{zr})_2
\end{aligned}\right\} \tag{30}$$

At $z = h_2$

$$\left.\begin{aligned}
-\,(\sigma_z)_{T_3} &= (\sigma_z)_3\\
-\,(\tau_{zr})_{T_3} &= (\tau_{zr})_3
\end{aligned}\right\} \tag{31}$$

Conditions (29) with the help of (14) - (17) and (21) - (24) we have,

$$\left.\begin{aligned}
A_1 &= A_1{}'\,A_0\\
B_1 &= B_1{}'\,A_0\\
C_1 &= C_1{}'\,A_0\\
D_1 &= D_1{}'\,A_0
\end{aligned}\right\} \tag{32}$$

where

$$A_1' = -C_1' = \frac{1}{\xi^2} \left[\frac{\beta_1 E_1}{2(1+\sigma_1)} + 2\xi B_1 \right]$$

$$B_1' = D_1' = \left[\mu_1 - \frac{E_1}{2(1+\sigma_1)} \right] \frac{\beta_1}{4(1-\sigma_1)\xi^2}$$

Using (14), (15), (25) and (26) on the conditions of (31) we have,

$$\left.\begin{aligned} A_3 &= A_3' \, A_0 \\ B_3 &= B_3' \, B_0 \end{aligned}\right\}$$ (33)

where

$$A_3' = \frac{2\sigma_3}{\xi} \, B_3$$

$$B_3' = \frac{\mu_3 \beta_3}{\xi^2}$$

From the conditions (30) with the help of (14) - (17) and (21) - (24) we have

$$\left.\begin{aligned} A_2 &= A_2' \, A_0 \\ B_2 &= B_2' \, A_0 \\ C_2 &= C_2' \, A_0 \\ D_2 &= D_2' \, A_0 \end{aligned}\right\}$$ (34)

where

$$A_2' = \frac{1}{2\xi p} \left[\{3(1-2\sigma_2) - 2\xi h_1\} p \, B_2 - (1-2\sigma_2) D_2 - S_3 \right]$$

$$B_2' = \frac{2(1-\sigma_2) S_5 - q_2 S_1}{2(1-\sigma_2)(q_1 - pq_2)}$$

$$C_2' = \frac{S_2 - pB_2 - (1 - 4\sigma_2 + 2\xi h_1) D_2}{2\xi}$$

$$D_2' = \frac{2(1 - \sigma_2) pS_5 - q_1 S_1}{2(1 - \sigma_2)(q_1 - pq_2)}$$

$$S_1 = \frac{(1 + 2\sigma_2) \mu_2 \beta_2 h_1}{2(1 + \sigma_2) \xi}$$

$$S_2 = \frac{(1 + 2\xi h_1) \mu_2 \beta_2}{\xi^2}$$

$$S_3 = \left[\frac{\mu_2 (1 + \xi h_1)}{\xi} - \frac{E_1 h_1}{2(1 + \sigma_2)}\right] \frac{\beta_2}{\xi}$$

$$S_4 = \left[\mu_2 - \frac{E_2 p}{2(1 + \sigma_2)}\right] \frac{\beta_2 (1 + \xi h_1)}{\xi^2}$$

$$S_5 = 2S_4 - (p - 1)^2 S_2$$

$$p = e^{2\xi h_1}$$

$$q_1 = (1 - 4\sigma_2 + 4p - p^2) p$$

$$q_2 = 2(p + 1 - 2\sigma_2) - (1 + 4\sigma_2)(p - 1)^2$$

The relations (32), (33) and (34) give ten constants A_1, B_1, C_1, D_1, A_2, B_2, C_2, D_2, A_3 and B_3 in terms of A_0. So the formal solution of the problem is completed.

The resultant stresses are in the direction of z-axis is

On $z = 0$,

$$\int_0^\infty r (\sigma_z)_{R_1} J_0 (\xi r) \, dr = \int_0^\infty r \left[(\sigma_r)_1 + (\sigma_z)_{T_1}\right] J_0 (\xi r) \, dr$$

$$= \left[2(1 - 2\sigma_1) \xi^2 B_1 - 2\xi^3 A_1 - \mu_1 \beta_1\right] A_0 \tag{35}$$

At $Z = h_1$,

$$\int_0^\infty r \, (\sigma_z)_{R_2} J_0 \, (\xi r) \, dr = \int_0^\infty r \Big[(\sigma_z)_2 + (\sigma_z)_{T_2} \Big] J_0 \, (\xi r) \, dr$$

$$= \Big[- \xi^3 \, A_2 \, e^{\xi h} + \xi^2 \, (1 - 2\sigma_2 - \xi h_1) \, e^{\xi h_1} \, B_2 + \xi^3 \, C_2 \, e^{-\xi h_1}$$

$$+ \xi^2 \, (1 - 2\sigma_2 + \xi h_1) \, D_2 \, e^{-\xi h_1} - \mu_2 \, \beta_2 \, (1 + \xi h_1) \, e^{-\xi h_1} \Big] A_0 \qquad (36)$$

At $Z = h_2$,

$$\int_0^\infty r \, (\sigma_z)_{R_3} J_0 \, (\xi r) \, dr = \int_0^\infty r \Big[(\sigma_z)_3 + (\sigma_z)_{T_3} \Big] J_0 \, (\xi r) \, dr$$

$$= \Big[(1 - 2\sigma_3) \, \xi^2 \, B_3 + (A_3 + B_3 \, h_2) \, \xi^3 - \mu_3 \, \beta_3 \, (1 + \xi h_2) \Big] e^{-\xi h_2} A_0 \qquad (37)$$

Thus, the total thermo-elastic stress $(\sigma_z)_R$ in the underlying mass is

$$\int_0^\infty r \, (\sigma_z)_R \, J_0 \, (\xi r) \, dr = \int_o^\infty r \Big[(\sigma_z)_{R_1} + (\sigma_z)_{R_2} + (\sigma_z)_{R_3} \Big] J_0 \, (\xi r) \, dr \qquad (38)$$

Flux of heat on the boundaries :

Let the flux of heat in a region of the surface $z = 0$, distributed through layers in the underlying mass be

$$\frac{\partial T}{\partial z} = f\Big(\frac{r}{a}\Big), \qquad 0 < r < a$$

$$= 0, \qquad\qquad r > a$$

Using dimensionless variables

$$\xi A_0 \, (\xi) = a \, \chi \, (\xi a), \qquad \eta = \xi a, \qquad \rho = \frac{r}{a}, \qquad \zeta = \frac{z}{a}$$

where a is some length and η, a new variable of integration, we get from (10) and (13), on $z = 0$

$$\frac{\partial T}{\partial z} = - \frac{1}{a} \int_0^\infty \eta \chi(\eta) J_0(\rho\eta) d\eta \tag{39}$$

the Hankel inversion theorem

$$\chi(\eta) = - \frac{1}{a} \int_0^1 \rho f(\rho) J_0(\rho\eta) d\eta \tag{40}$$

For a simple physical situation we consider a linear temperature distribution $f(\rho) = K\rho$, K = constant, then from (40)

$$\chi(\eta) = - \frac{K}{a\eta} J_1(\eta)$$

With this value of $\chi(\eta)$, the problem is completely solved since only unknown $A_0(\xi)$ is now known.

Numerical Results :

If the upper layer be concrete pavement, the middle layer be gravel base and the underlying mass be natural soil then elastic constants for those materials are[4]

$E_1 = 2.18 \times 10^5$ g/cm^2, $E_2 = 1.1 \times 10^8$ g/cm^2, $E_3 = 0.4 \times 10^8$ g/cm^2

$\alpha_1 = 5 \times 10^{-6}/°C$, $\alpha_2 = 7.5 \times 10^{-6}/°C$, $\alpha_3 = 2.3 \times 10^{-6}/°C$,

$\mu_1 = 0.94 \times 10^8$ g/cm^2, $\mu_2 = 0.43 \times 10^8$ g/cm^2, $\mu_3 = 0.14 \times 10^8$ g/cm^2

$\sigma_1 = 0.15$, $\sigma_2 = 0.25$ $\sigma_3 = 0.5$

$K_1 = 6.4 \times 10^{-3}$, $K_2 = 6.7 \times 10^{-3}$, $K_3 = 2.9 \times 10^{-3}$

So, evaluating constants for a given value of η when $a=1$, and $h_1=2$, $h_2=4$, we have

$A_1 = -1471.9$, $B_1 = -1.557$, $C_1 = -1471.59$, $D_1 = -1.557$

$A_2 = -46.43$, $B_2 = -34.90$, $C_2 = -6967.67$, $D_2 = -2335.59$

$A_3 = -85.56$, $B_3 = -85.56$

So applying dimensionless variables on (38) substituting the value of $\chi(\eta)$ from (41) and the values of constants in (38), we get

$$\int_0^\infty \rho (\sigma_{z)_R} J_0 (\rho\eta)\, d\rho = -\, 2709.43 \, \frac{K}{\eta^2} \, J_1 (\eta)$$

whose Hankel inverse transform is

$$(\sigma_z)_R = -\, 2709.43 \times K \int_0^\infty \frac{J_1 (\eta) \, J_0 (\rho\eta)}{\eta} \cdot d\eta$$

$$= -\, 2709.43 \times K \times F\left(\frac{1}{2}, \frac{1}{2}, 1; \rho^2\right), \qquad \rho < 1$$

$$= -\, 2709.43 \times K \times \frac{2}{\pi}, \qquad\qquad \rho < 1$$

$$= -\, 2709.43 \times K \, \frac{1}{2} \, E\left(\frac{1}{2}, \frac{1}{2}; 2; \frac{1}{\rho^2}\right) \qquad \rho > 1$$

F denotes hypergeometric function.

Acknowledgements

References

1. Burmister, D.M. (1945) *J. Appl. Phys.* **16**(5) : 296.

2. Nowacki, W. (1986) *Thermoelasticity*, 2nd edn., Pergamon Press, p. 41.

3. Paria, G. (1956) *Bull. Cal. Math. Soc* **48** : 73.

4. (1972) *International Critical Table of Numerical Data*, N.R.C., U.S.A., McGraw-Hill Book. Co., Inc., New York.

5. Love, A.E.H. (1927) *A Treatise on the Mathematical Theory of Elasticity*, 4th edn., Dover Publication, p. 276.

6. Snedden, I.N. (1951) *Fourier Transforms*, McGraw-Hill Book Co., Inc., New York.

7. Waston, G.N. (1978) *A Treatise on the Theory of Bessel Functions*, 2nd edn., C.U.P.

Effect of rotation on thermal instability in Walters elastico-viscous fluid

PARDEEP KUMAR

Department of Mathematics, Himachal Pradesh University, Summer Hill, Shimla 171 005, India

Abstract

The thermal instability of a layer of Walters elastico-viscous fluid (Model B') acted on by a uniform rotation is considered. For stationary convection, Walters elastico-viscous fluid behaves like a Newtonian fluid. It is found that rotation has a stabilizing effect and presence of each-rotation and viscoelasticity introduces oscillatory modes which were non-existent in their absence. The sufficient condition for the non-existence of overstability is also obtained.

(Keywords : thermal instability/ Walters elastico-viscous fluid (Model B')/ uniform rotation).

Introduction

The thermal instability of a fluid layer with maintained temperature gradient by heating the underside, plays an important role in geophysics, interior of the earth, oceanography and the atmospheric physics etc. and has been investigated by several authors. A detailed account of the thermal convection in Newtonian fluids in the presence of uniform rotation has been discussed exhaustively by Chandrasekhar.[1] Vest and Arpaci[2] have studied the stability of a horizontal layer of Maxwell's viscoelastic fluid heated from below. Bhatia and Steiner[3] have considered the effect of a uniform rotation on the thermal instabilty of a viscoelastic (Maxwell) fluid and have found that rotation has a destabilizing influence in contrast to the stabilizing effect on Newtonian fluid. Sharma[4] has studied the thermal instability of a layer of viscoelastic (Oldroydian) fluid acted on by a uniform rotation and found that rotation has destabilizing as well as stabilizing effects under certain conditions in contrast to that of a Maxwell fluid where it has a destabilizing effect.

There are many elastico-viscous fluid that cannot be characterized by Maxwell's constitutive relations or Oldroyd's[5] constitutive relations. One such class of elastico-viscous fluid is Walters fluid (Model B'). Chakraborty and Sengupta[6] have studied the flow of unsteady viscoelastic (Walters liquid B') conducting fluid through two porous concentric non-conducting infinite circular cylinders rotating with different angular velocities in the

presence of a uniform axial magnetic field. In another study, Sharma and Kumar[7] have studied the steady flow and heat transfers of Walters fluid (Model B') through a porous pipe of uniform circular cross-section with small suction. It is this class of elastico-viscous fluids we are interested in particularly the thermal convection in such fluids in the presence of rotation.

The present paper, therefore, attempts to study the thermal instability in Walters elastico-viscous fluid (Model B') in presence of uniform rotation.

Formulation of the Problem and Dispersion Relation

Consider an infinite horizontal layer of Walters elastico-viscous fluid (Model B') of depth d which is acted on by a uniform rotation $\vec{\Omega}$ (0, 0, Ω) and gravity force $\vec{g}$ (0, 0, –g). This layer is heated from below so that a steady adverse temperature gradient $\beta(= |\, dT / dz\, |)$ is maintained. The equations of motion, continuity and heat conduction governing the flow of Walters elastico-viscous fluid in the presence of rotation are :

$$\frac{\partial \vec{q}}{\partial t} + (\vec{q} \cdot \nabla)\, \vec{q} = -\frac{1}{\rho_0}\, \nabla p + \left(\nu - \nu' \frac{\partial}{\partial t} \right) \nabla^2 \vec{q} + \vec{g} \left(1 + \frac{\delta \rho}{\rho_0} \right) + 2\, (\vec{q} \times \vec{\Omega}), \qquad (1)$$

$$\nabla \cdot \vec{q} = 0, \qquad (2)$$

$$\frac{\partial T}{\partial t} + (\vec{q} \cdot \nabla)\, T = \chi\, \nabla^2\, T, \qquad (3)$$

where $\vec{q}(u, v, w)$, p, ρ, T, ν, ν' and χ are respectively the velocity, pressure, density, temperature, kinematic coefficient of viscosity, kinematic viscoelasticity and thermal diffusivity. The equation of state for the fluid is

$$\rho = \rho_0 \left[1 - \alpha\, (T - T_0) \right] \qquad (4)$$

where ρ_0, T_0 are respectively, the density and temperature of the fluid at the reference level $z = 0$ and α is the coefficient of thermal expansion.

Here we make the Boussinesq approximation under which the density changes may be disregarded in all terms in the equations of motion except the one in the external force.

The initial state is one in which the velocity, density, pressure and temperature at any pont in the fluid are respectively given by

$$\vec{q} = (0, 0, 0), \quad \rho = \rho(z), \quad p = p(z) \text{ and } T = T(z) \tag{5}$$

Let $\vec{q}(u, v, w)$ $\delta\rho$, δp and θ denote respectively the perturbation in velocity $(0,0,0)$, density ρ, pressure p and temperature T. Then the linearized perturbation equations are

$$\frac{\partial \vec{q}}{\partial t} = -\frac{1}{\rho_0} \nabla \delta p + \left(\nu - \nu' \frac{\partial}{\partial t}\right) \nabla^2 \vec{q} + \vec{g}\frac{\delta\rho}{\rho_0} + 2 (\vec{q} \times \vec{\Omega}), \tag{6}$$

$$\nabla \cdot \vec{q} = 0, \tag{7}$$

$$\frac{\partial \theta}{\partial t} + (\vec{q} \cdot \nabla) T = \chi \nabla^2 \theta. \tag{8}$$

Within the framework of Boussinesq approximation, eqn(6)-(8) becomes

$$\frac{\partial \nabla^2 w}{\partial t} - g\alpha\left(\frac{\partial^2\theta}{\partial x^2} + \frac{\partial^2\theta}{\partial y^2}\right) + 2\Omega\frac{\partial\zeta}{\partial z} = \left(\nu - \nu'\frac{\partial}{\partial t}\right)\nabla^4 w, \tag{9}$$

$$\frac{\partial\zeta}{\partial t} - 2\Omega\frac{\partial w}{\partial z} = \left(\nu - \nu'\frac{\partial}{\partial t}\right)\nabla^2\zeta, \tag{10}$$

$$\left(\frac{\partial}{\partial t} - \chi\nabla^2\right)\theta = \beta w, \tag{11}$$

where $\nabla^2 = \left(\dfrac{\partial^2}{\partial x^2} + \dfrac{\partial^2}{\partial y^2} + \dfrac{\partial^2}{\partial z^2}\right)$ and $\zeta = \dfrac{\partial v}{\partial x} - \dfrac{\partial u}{\partial y}$ denotes the z-component of vorticity.

We now analyze the disturbances into normal modes, assuming that the perturbation quantities are of the form

$$[w, \theta, \zeta] = [W(z), \Theta(z), Z(z)] \exp(ik_x x + ik_y y + nt), \tag{12}$$

where k_ι, k_ι are wave numbers along x and y directions respectively, $k^2 = k_x^2 + k_y^2$ and n is, in general, a complex constant.

Letting

$$a = kd, \quad \sigma = \frac{nd^2}{\nu}, \quad p_1 = \frac{\nu}{x},$$

$$(x, y, z) \rightarrow (\hat{x}d, \hat{y}d, \hat{z}d) \quad \text{and} \quad F = \frac{\nu'}{d^2}.$$

Equations (9)-(11) using expression (12) give

$$\left[\sigma (D^2 - a^2) W + \left(\frac{g\alpha d^2}{\nu}\right) a^2 \Theta + \left(T_A^{1/2} d\right) Dz\right] = (1 - F\sigma)(D^2 - a^2) W, \tag{13}$$

$$\left[(1 - F\sigma)(D^2 - a^2) - \sigma\right] z = -\frac{T_A^{i/2}}{d} DW, \tag{14}$$

$$[D^2 - a^2 - p_i \sigma] \Theta = -\left(\frac{\beta d^2}{\chi}\right) W, \tag{15}$$

where $T_A = \frac{4\Omega^2 d^4}{\nu^2}$ denotes the Taylor number and $D = \frac{d}{dz}$.

Applying the operator $[D^2 - a^2 - p_1 \sigma][(1 - F\sigma)(D^2 - a^2) - \sigma]$ to eqn. (13), we eliminate Θ and z to obtain

$$\sigma (D^2 - a^2)(D^2 - a^2 - p_1 \sigma)\left[(1 - F\sigma)(D^2 - a^2) - \sigma\right] W$$

$$- R a^2 \left[(1 - F\sigma)(D^2 - a^2) - \sigma\right] W - T_A (D^2 - a^2 - p_1 \sigma) D^2 W = (1 - F\sigma)$$

$$(D^2 - a^2 - p_1 \sigma)(D^2 - a^2)^2 \left[(1 - F\sigma)(D^2 - a^2) - \sigma\right] W, \tag{16}$$

where $R = \dfrac{g\alpha\beta d^4}{\nu\chi}$ stands for Rayleigh number.

We now assume that the fluid layer is confined between two free boundaries. The case is of artificial nature but due to mathematical simplicity it enables us to show the behaviour of rotation on Walters elastico-viscous fluid analytically. Then the boundary conditons appropriate for the problem are

$$W = D^2 W = 0', \quad \Theta = 0', \quad DZ = 0 \quad \text{at} \quad \hat{z} = 0 \quad \text{and} \quad \hat{z} = 1. \tag{17}$$

Dropping the caps for convenience and using the above boundary conditions, it can be shown that all the even order derivatives of W must vanish on the boundaries and hence the proper solution of eqn. (16) characterizing the lowest mode is

$$W = W_0 \sin \pi z \ , \tag{18}$$

where W_0 is a constant.

Substituting (18) in eqn. (16), we obtain the dispersion rotation

$$R_i = \frac{(1+x)(1+x+i\,p_1\,\sigma_1)\,((1-i\,\sigma_1\,\pi^2\,F)\,(1+x)+i\,\sigma_i)}{\cfrac{((1-i\,\sigma_i\,\pi^2\,F)\,(1+x)+i\,\sigma_1)+T_i\,(1+x+i\,p_1\,\sigma_1)}{x\,[(1-i\,\sigma_1\,\pi^2\,F)\,(1+x)+i\,\sigma_1]}} \tag{19}$$

where

$$R_1 = \frac{R}{\pi^4} \ , \quad T_1 = \frac{T_A}{\pi^4} \ , \quad a^2 = \pi^2 x \ , \quad \frac{\sigma}{\pi^2} = i\,\sigma_i \ ,$$

it being remembered that σ can be complex.

Here we consider the overstable mode and so σ_1 is real in eqn. (19).

For the case of stationary convection i.e. $\sigma = 0$. eqn. (19) reduces to

$$R_1 = \frac{(1 + x)^3 + T_1}{x} \quad , \tag{20}$$

[a result given by Chandrashekhar[1]. eqn(130), p. 95].

We thus find that for the stationary convection, the visco- elasticity parameter F vanishes with σ and Walters elastico-viscous fluid behaves like an ordinary Newtonian fluid.

To study the effect of rotation, we examine the nature of dR_1/dT_1. From eqn. (19), it follows that

$$\frac{dR_1}{dT_1} = \frac{(1 + x + \dot{\iota}\, p_1\, \sigma_1)}{x\,[(1 - \dot{\iota}\, \sigma_1\, \pi^2\, F)\,(1 + x) + \dot{\iota}\, \sigma_1]} \tag{21}$$

On equating real and imaginary parts of eqn. (21), it follows that

$$\frac{dR_1}{dT_1} = \frac{1}{x} \quad , \tag{22}$$

which is always positive. The rotation thus has a stabilizing influence.

Stability of the System and Oscillatory Modes

Multiplying eqn. (13) by $W*$, the complex conjugate of W, integrating over the range of z and making use of eqn. (14) and (15) together with the boundary conditions (17), we obtain

$$- \sigma I_1 + \frac{g\alpha\chi a^2}{\nu\beta}\,(I_2 + p_1\, \sigma^*\, I_3) - d^2(1 - F\sigma^*)\,I_4 - d^2\, \sigma^*\, I_5 = (1 - F\sigma)\,I_\sigma\,, \tag{23}$$

where

$$I_1 = \int_0^1 \left(|DW|^2 + a^2\,|W|^2\right) dz\,, \quad I_2 = \int_0^1 \left(|D\Theta|^2 + a^2\,|\Theta|^2\right) dz\,,$$

$$I_3 = \int_0^1 |\Theta|^2 \, dz \; , \qquad I_4 = \int_0^1 \left(|Dz|^2 + a^2 |z|^2 \right) dz \; ,$$

$$I_5 = \int_0^1 |z|^2 \, dz \; , \qquad I_6 = \int_0^1 \left(|D^2 W|^2 + 2 a^2 |DW|^2 + a^4 |W|^2 \right) dz \; , \qquad (24)$$

and σ^* is the complex conjugate of σ. The integrals $I_1 - I_6$ are all positive definite. Putting $\sigma = \sigma_r + i \, \sigma_i$ in eqn. (23) and equating the real and imaginary parts, we obtain

$$\sigma_r \left[-I_1 + \frac{g \alpha \chi a^2}{\nu \beta} \, p_1 I_3 + d^2 F I_4 - d^2 I_5 + F I_6 \right] = - \frac{g \alpha \chi a^2}{\nu \beta} \, I_2 + d^2 I_4 + I_6 \; , \qquad (25)$$

and

$$\sigma_1 \left[I_1 + \frac{g \alpha \chi a^2}{\nu \beta} \, p_1 I_3 + d^2 F I_4 - d^2 I_5 - F I_6 \right] = 0 \quad , \qquad (26)$$

It is evident from eqn. (25) that σ_r is positive or negative. The system is therefore stable or unstable. It is clear from eqn. (26) that rotation and viscoelasticity introduce oscillatory modes in the system which were non-existent in their absence.

The Case of Overstability

Here we discuss the possibility of whether instability may occur as an overstability. When the marginal state is oscillatory, we must have $\sigma_r = 0$. $\sigma_i \neq 0$.

Since for overstability, we wish to determine the critical Rayleigh number for the onset of instability *via* a state of pure oscillations, it will suffice to find conditions for which eqn. (19) will admit of solutions with σ_r real.

Separating the real and imaginary parts of eqn. (19), we have

$$R_1 (\alpha - 1) = \alpha^3 - \alpha \sigma_1^2 \left[(\pi^2 F \alpha - 1)(\pi^2 F \alpha - 1 - 2 p_1) \right] + T_1 \; , \qquad (27)$$

$$R_1 (\alpha - 1)(1 - \pi^2 F \alpha) = (1 - \pi^2 F \alpha) \, \alpha \, [2\alpha^2 - \sigma_1^2 p_1 (1 - \pi^2 F \alpha)]$$

$$+ p_1 (\alpha^3 + T_1) \; , \qquad (28)$$

where $1 + x = \alpha$.

Eliminating R_1 between eqn. (27) and (28), we have

$$[(1 - \pi^2 F\alpha)^2 \, \alpha \, (1 + p_1 - \pi^2 \, F \, \alpha)] \, \sigma_1^2 + [\alpha^3 \, (1 + p_1 - \pi^2 \, F \, \alpha) - T_1 \, (1 - p_1 - \pi^2 F\alpha) = 0. \quad (29)$$

Eqn. (29) is of the form

$$A \, \sigma_1^2 + B = 0 \, . \quad (30)$$

where A, B are coefficient of σ_1^2 and constant term respectively in eqn. (29). As σ_1 is real for overstability, the values of σ_1^2 is positive. Eqn. (30) shows that this is impossible if $A > 0$ and $B > 0$. Therefore, $A > 0$ and $B > 0$ gives sufficient conditions for the non-existence of overstability, which yields

$$p_1 > \pi^2 F \alpha - 1 \qquad \text{and} \qquad p_1 < 1 - \pi^2 F \alpha \quad . \quad (31)$$

which further implies that

$$F (\pi^2 + k^2 d^2) - 1 \; < \; \frac{\nu}{\chi} \; < \; 1 - F (\pi^2 + k^2 d^2) \quad (32)$$

Thus for $F (\pi^2 + k^2 d^2) - 1 < \dfrac{\nu}{\chi} < 1 - F (\pi^2 + k^2 d^2)$, overstability cannot occur. The condition (32) is, therefore, sufficient condition for the non-existence of overstability, the violation of which does not necessarily imply occurrence of overstability.

Acknowledgement

References

1. Chandrasekhar, S. (1961) *Hydrodynamic and Hydromagnetic Stability*, Dover Publication, N.Y.

2. Vest, C.M. & Arpaci, V.S. (1969) *J. Fluid Mech.* **36** : 613.

3. Bhatia, P.K. & Steiner, J.M. (1972) *Z. Angew Math. Mech.* **52** : 321.

4. Sharma, R.C. (1976) *Acta Phys. Hung.* **40** : 11.

5. Oldroyd, J.G. (1958) *Proc. Roy Soc. (London)* **A245** : 278.

6. Chakraborty, G. & Sengupta, P.R. (1994) *Proc. Nat. Acad. Sci. India* **64A** : 75.

7. Sharma, P.R. & Kumar, H. (1995) *Proc. Nat. Acad. Sci. India* **65A** : 75.

.

Possibility of the simultaneous occurrence of potential minima along two crystallographic directions in an octahedral potential

R.K. TIWARI* and PREM N. SINGH**

*Department of Physics and Electronics, Dr. R.M.L. Awadh University, Faizabad - 224 001, India

**Department of Physics, Rana Pratap P.G. College, Sultanpur - 228 001, India

*Author of correspondence.

Abstract

Within the framework of two parameter octahedral potential for a dipolar impurity in ionic crystals, it is possible for impurity to possess minimum-energy orientational configurations in two crystallographic directions simultaneously. Two possible combinations are <111>–<110> and <111> – <100>. Taking second model here we have tried to findout the expressins for polarization.

(**Keywords :** ionic crystals/octahedral potential/polarization)

Introduction

Diatomic and off-centred monoatomic impurities in crystals with octahedral symmetry have attracted considerable attention. Within limit of infinite potential barriers these impurities align themselves along certain preferred crystallographic directions. In case of finite potential barriers, they tunnel between the equilibrium oriential configurations resulting in interesting electrical, thermal and optical properties. The above mentioned properties, depend critically on the actual minimum - energy orientational configurations of the impurity, apart from certain other parameters such as the height of the potential barriers etc. The simplest form of the octahedral potential for the angular motion of diatomic impurity in solid-state matrices was first presented by Devonshire[1] and is given by :

$$V(\theta, \alpha) = - (5K/2) \ [(x^4 + y^4 + z^4) / r^4] \qquad (1)$$

where $x/r = \sin\theta \cos\alpha$, $y/r = \sin\theta \sin\alpha$ and $z/r = \cos\theta$. Many experimental results for systems such as OH^- and CN^- ions in alkali halide matrices[2,3] and impurities like HCl,

HBr etc. in rare gas matrices[4,5] have successfully intepreted in terms of this one-parameter Devonshire potential. It is easy to show that for this potential the minimum-energy orientational configuration for the impurity are along one of six <100> directions and along one of the eight <111> directions if K is positive and negative respectively. A <110> minimum-energy configuration was not possible within the framework of the Devonshire potential This potential in fact, retains only the first significant term (the $L = 4$ term) in the expansion of octahedral potential. To make it for the <110> configuration, the next term (the $L=6$ term) was added to make the two parameter octahedral potential as given by

$$V(\theta, \alpha) = -(5K/2) \ [(x^4 + y^4 + z^4)/r^4] + (1/2)K^l \ [180 \ (x^2 \ y^2 \ z^2/r^6) - (15/r^6)$$

$$(x^2 \ y^4 + x^2 \ z^4 + y^2 \ z^4 + z^2 \ x^4 + z^2 \ y^4) + (2/r^6) \ (x^6 + y^6 + z^6)] \qquad (2)$$

It was concluded in a previous communcation[6] that if $(10/21) < (K^l/K) < (-20/189)$, a <110> equilibrium orientational configuration is physically possible. This was also subscribed later by Beyeler[7] whose condition was $26° < \alpha < 173°$, where $\alpha = \tan^{-1} (K^l/K)$.

The nature of Li^+ in KCl matrix are explained by single tunneling model proposed by Gomez $et\ al.$[9] but not well applied for other's as $NaBr{:}F^-$ and $RbCl{:}CN^-$ systems. Various attempts[6,7] to explain the experimental data were made using <110> model, but got limited success. Experimental results of $RbCl{:}CN^-$ system were not explained using this model. This system was also not very well explained in terms of the <110> and <111> model proposed by Pandey $et\ al.$[8] In the present paper we have attempted to find out the expression of polarization of <100> and <111> model.

Limitations of Old Models and Scope of Simultaneous Potential Minima in two Crystallographic Directions

Inspite of KCL:Li^+ system, which shows agreement with the <111> off-centred model of Gomez $et\ al.$[9], many other paraelectric systems present difficulty in understanding the various experiments associated with them. In those cases existence of two sets of minimum-energy orientational configurations of the impurity in the matrix give interesting and exciting results. Initial experiments of Seward and Narayanmurti[3] presented evidence that impurity could have potential minima along any of the six <100> directions. Using the model RbCl:CN^- system, paraelectric resonance[10] and specific heat[11] at low temperature could not be explained. However, Luty[12] and Beyeler[13] on stress-induced splitting of the
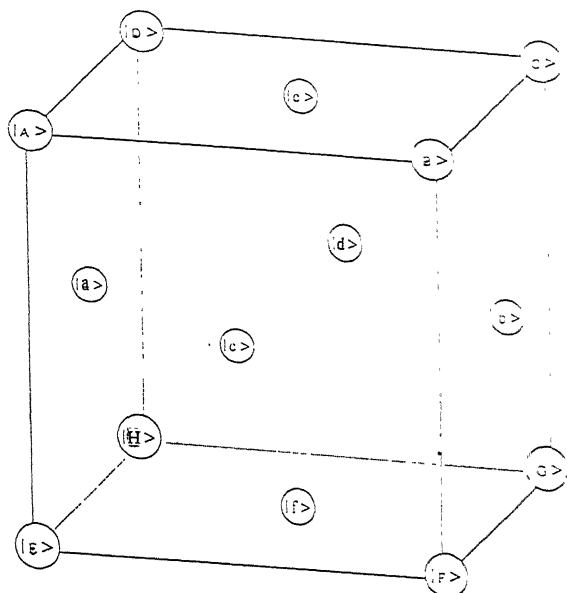
Fig. 1 – Pocket states for simultaneous potential minima along the <111> and <100> directions in the O_h symmetry group.

intramolecular vibrational line showed that correct minimum-energy orientational configuration of CN⁻ impurity in ionic crystals was along one of eight <111> directions. The model fails to explain the double bump in specific heat results of RbCl:CN⁻ system.

Similarly, the calculation of Quigley and Das[14] shows minima position along <111> direction while the high field polarization and paraelectric cooling experiments of the Rollefson[15] are better fitted along the <110> direction. After some time Rollefson[16] suggested the existence of potential minima along the <111> direction, which are only slightly less deep than the <110> minima. This thing is physically possible even within the framework of the two-parameter potential of eqn. (2) discussed above. Specific heat anomaly at low temperatures was not fully explained within the simple <110> model. There are several examples which could not be fully explained by simple tunneling model. At very low temperatures, when most of the molecules remain in lower well, the behaviour of system can easily be explained in terms of simple model. But at elevated temperatures, more and more molecules are transferred to the upper well and the system shows a marked departure. In some cases when both wells are equally deep, the behaviour of the system becomes crucially linked to the experimental conditions and one gets controversial results.

Theory

There were six equivalent <100>, the eight <111> and twelve <110> states in paper of Gomez et al.[9] In present case there is a set of each of six and eight equivalent states for the case of the simultaneous occurrence of the potential minima along the <100> and <111> directions. The designation of states is given in Fig. 1.

For a finite crystal field, there will be matrix elements of the Hamiltonian connecting the different states i.e., there will be a finite probability of tunneling through the potential barrier to a new orientation. There will be matrix element connecting the states, for example, $|A>$ of the <111> minima group to the nearest neighbouring wells $|B>$, $|D>$ and $|E>$ of the same minima group. Similarly, there will be equal matrix element connecting the states $|a>$ of the <100> minima group to the states $|c>$, $|d>$, $|e>$ and $|f>$ of the same group. Here we assume that the tunneling matrix elements of the far off well are insignificant compared to the tunneling matrix elements to the nearest-neighbouring wells. Now impurity can tunnel from a well of the <111> group of the nearest-neighbour well of the <100> group. Thus we have equal matrix element of the Hamiltonian connecting the states $|A>$ of the <111> group of the states $|a>$, $|c>$ and $|e>$ of the <100> group.

Explanation of Field Polarization Effect

If we apply an external field E at an angle θ with the dipole orientation, then the average field polarization (P) in the field direction is given by

$$P = N\mu \; \frac{\sum\limits_{r=1}^{n} \cos\theta_r \; e^{\mu E \cos\theta_r /kT}}{\sum\limits_{r=1}^{n} e^{\mu E \cos\theta_r /kT}} \tag{3}$$

where k = Boltzmann Constant, T = Absolute temperature, N = Dipole concentration, μ = Dipole moment.

Let $x = \dfrac{\mu E}{kT}$. So eqn. (3) takes the form

Table 1 – Values of $\cos\theta r$ and corresponding dipolar energy for <100> system with applied electric field in <100> direction.

Well	100	100	010	010	001	001
$\cos\theta r$	1	−1	0	0	0	0
$-\mu E\cos\theta r$	$-\mu E$	μE	0	0	0	0

Table 2 – Values of $\cos\theta r$ and corresponding dipolar energy for <100> system with applied electric field in <110> direction.

Wells	100	100	010	010	001	001
$\cos\theta r$	$1/\sqrt{2}$	$-1/\sqrt{2}$	$1/\sqrt{2}$	$-1/\sqrt{2}$	0	0
$-\mu E\cos\theta r$	$-\mu E/\sqrt{2}$	$\mu E/\sqrt{2}$	$-\mu E/\sqrt{2}$	$\mu E/\sqrt{2}$	0	0

Table 3 – Values of $\cos\theta r$ and corresponding dipolar energy for <100> system with applied electric field in <111> direction.

Wells	100	100	010	010	001	001
$\cos\theta r$	$1/\sqrt{3}$	$-1/\sqrt{3}$	$1/\sqrt{3}$	$-1/\sqrt{3}$	$1/\sqrt{3}$	$-1/\sqrt{3}$
$-\mu E\cos\theta r$	$-\mu E/\sqrt{3}$	$\mu E/\sqrt{3}$	$-\mu E/\sqrt{3}$	$\mu E/\sqrt{3}$	$-\mu E/\sqrt{3}$	$\mu E/\sqrt{3}$

Table 4 – Values of $\cos\theta r$ and corresponding dipolar energy for <100>+<111> system with applied electric field in <100> direction.

Wells	100	100	010	010	001	001	111	111	111	111	111	111	111	111
$\cos\theta r$	1	−1	0	0	0	0	$1/\sqrt{3}$	$1/\sqrt{3}$	$1/\sqrt{3}$	$-1/\sqrt{3}$	$1/\sqrt{3}$	$-1/\sqrt{3}$	$-1/\sqrt{3}$	$-1/\sqrt{3}$
$-\mu E\cos\theta r$	$-\mu E$	μE	0	0	0	0	$-\mu E/3$	$-\mu E/3$	$-\mu E/3$	$\mu E/3$	$-\mu E/3$	$\mu E/3$	$\mu E/3$	$\mu E/3$

Table 5 – Values of $\cos\theta r$ and corresponding dipolar energy for <100>+<111> system with applied electric field in <100> direction.

Wells	100	100	010	010	001	001	111	111	111	111	111	111	111	111
$\cos\theta r$	$1/\sqrt{2}$	$-1/\sqrt{2}$	$1/\sqrt{2}$	$-1/\sqrt{2}$	0	0	$2/\sqrt{6}$	$2/\sqrt{6}$	0	0	0	0	$-2/\sqrt{6}$	$-2/\sqrt{6}$
$-\mu E\cos\theta r$	$-\mu E/\sqrt{2}$	$\mu E/\sqrt{2}$	$-\mu E/\sqrt{2}$	$\mu E/\sqrt{2}$	0	0	$-2\mu E/\sqrt{6}$	$-2\mu E/\sqrt{6}$	0	0	0	0	$2\mu E/\sqrt{6}$	$2\mu E/\sqrt{6}$

Table 6 – Values of $\cos\theta_r$ and corresponding dipolar energy for <100>+<111> system with applied electric field in <111> direction.

Wells	100	100	010	010	001	001	111	111	111	111	111	111	111	111
$\cos\theta_r$	$1/\sqrt{3}$	$-1/\sqrt{3}$	$1/\sqrt{3}$	$-1/\sqrt{3}$	$1/\sqrt{3}$	$-1/\sqrt{3}$	1	$1/3$	$1/3$	$1/3$	$-1/3$	$-1/3$	$-1/3$	-1
$-\mu E\cos\theta_r$	$-\mu E/\sqrt{3}$	$\mu E/\sqrt{3}$	$-\mu E/\sqrt{3}$	$\mu E/\sqrt{3}$	$-\mu E/\sqrt{3}$	$\mu E/\sqrt{3}$	$-\mu E$	$-\mu E/3$	$-\mu E/3$	$-\mu E/3$	$\mu E/3$	$\mu E/3$	$\mu E/3$	μE

Table 7 – Expressions for polarization for the simple <100> off-centred model and the present model of simultaneous potential minima along the <100> and <111> directions. Here $x = \mu E/kT$ and the asterisk denotes experssions which represent saturation value for the case $x > 1$ (i.e., for larger field).

Direction of applied electric field	Polarization as expected from the simple <100> model	Polarization as expected from present model
<100>	$P = N\,\dfrac{e^x - e^{-x}}{4 + e^x + e^{-x}}$	$P = N\,\dfrac{\mu_1(e^{x_1} - e^{-x_1}) + \sqrt{3}\,\mu_2(e^{x_2/\sqrt{3}} - e^{-x_2/\sqrt{3}})}{4 + e^{x_1} + e^{-x_1} + 3(e^{x_2/\sqrt{3}} + e^{-x_2/\sqrt{3}})}$
	$P = N\mu^*$	$P = N\mu_1^*$
<110>	$P = N\mu\sqrt{2}\,\dfrac{e^{x/\sqrt{2}} - e^{-x/\sqrt{2}}}{1 + e^{x/\sqrt{2}} + e^{-x/\sqrt{2}}}$	$P = N\,\dfrac{(\mu_1/\sqrt{2})(e^{x_1/\sqrt{2}} - e^{-x_1/\sqrt{2}}) + (\sqrt{2}/3)\mu_2(e^{2x_2/\sqrt{6}} - e^{-2x_2/\sqrt{6}})}{3 + e^{x_1/\sqrt{2}} + e^{-x_1/\sqrt{2}} + e^{2x_2/\sqrt{6}} + e^{-2x_2/\sqrt{6}}}$
	$P = \dfrac{N\mu^*}{\sqrt{2}}$	$P = \dfrac{N\mu^*}{2}$
<111>	$P = N\mu\sqrt{3}\,\dfrac{e^{x/\sqrt{3}} - e^{-x/\sqrt{3}}}{e^{x/\sqrt{3}} + e^{-x/\sqrt{3}}}$	$P = N\,\dfrac{\sqrt{3}\,\mu_1(e^{x_1/\sqrt{3}} - e^{-x_1/\sqrt{3}}) + \mu_2(e^{x_2} - e^{-x_2} + e^{x_2/3} - e^{-x_2/3})}{3(e^{x_1/\sqrt{3}} + e^{-x_1/\sqrt{3}}) + e^{x_2} + e^{-x_2} + 3(e^{x_2/3} + e^{-x_2/3})}$
	$P = \dfrac{N\mu^*}{\sqrt{3}}$	$P = N\mu_2^*$

$$P = N\mu\,\frac{\displaystyle\sum_{r=1}^{n} \cos\theta_r\, e^{x\cos\theta_r}}{\displaystyle\sum_{r=1}^{n} e^{x\cos\theta_r}} \tag{4}$$

Now using eqn. (4) we find expression for polarization P in different cases.

Case 1 : System <100> and electric field along <100> direction : For <100> system with electric field in <100> direction value of $\cos\theta_r$, and their dipolar energy is given in Table 1. So using Table 1 and eqn. (4) we have expression for polarization given as

$$P = N\mu \; \frac{e^x - e^{-x}}{4 + e^x + e^{-x}}$$

(5)

For $x \gg 1$ (i.e., $\mu E \gg kT$)

$$P_s = N\mu$$

(6)

where P_s is saturation polarization.

Case 2 : System <100> and electric field along <110> direction : Using Table 2 and eqn. (4) we have expression for polarization given as

$$P = N\mu \; \frac{2\,[1/\sqrt{2})\,(e^{x/\sqrt{2}} - e^{-x/\sqrt{2}})]}{2 + 2\,(e^{x/\sqrt{2}} + e^{-x/\sqrt{2}})}$$

$$P = N\mu/\sqrt{2} \; \frac{e^{x/\sqrt{2}} - e^{-x/\sqrt{2}}}{1 + e^{x/\sqrt{2}} + e^{-x/\sqrt{2}}}$$

(7)

For $x \gg 1$ (i.e., $\mu E \gg kT$)

$$P_s = N\mu/\sqrt{2}$$

(8)

Case 3 : System <100> and electric field along <111> direction : Using Table 3 and eqn. (4) we have expression for polarization given as

$$P = N\mu \; \frac{3[(1/\sqrt{3})\,(e^{x/\sqrt{3}} - e^{-x/\sqrt{3}})]}{3(e^{x/\sqrt{3}} + e^{-x/\sqrt{3}})}$$

$$P = N\mu/\sqrt{3} \; \frac{e^{x/\sqrt{3}} - e^{-x/\sqrt{3}}}{e^{x/\sqrt{3}} + e^{-x/\sqrt{3}}}$$

(9)

For $x \gg 1$ (i.e., $\mu E \gg kT$)

$$P_s = N\mu/\sqrt{3} \tag{10}$$

Now we have extended our calculation to find out the expressions for polarization for system $\langle 100 \rangle + \langle 111 \rangle$ (present model).

Let μ and μ_2 be the dipole moment for $\langle 100 \rangle$ and $\langle 111 \rangle$ wells respectively.

Case 4 : System $\langle 100 \rangle + \langle 111 \rangle$ and electric field along $\langle 100 \rangle$ direction : Using Table 4 and eqn. (4) we have expression for polarization given as

$$P = N \; \frac{\mu_1 (e^{x_1} - e^{-x_1}) + 3\left\{(\mu_2/\sqrt{3}) (e^{x_2/\sqrt{3}} - e^{-x_2/\sqrt{3}})\right\}}{4 + e^{x_1} + e^{-x_1} + 3(e^{x_2/\sqrt{3}} + e^{-x_2/\sqrt{3}})}$$

$$P = N \; \frac{\mu_1 (e^{x_1} - e^{-x_1}) + \sqrt{3}\,\mu_2 (e^{x_2/\sqrt{3}} - e^{-x_2/\sqrt{3}})}{4 + e^{x_1} + e^{-x_1} + 3 (e^{x_2/\sqrt{3}} + e^{-x_2/\sqrt{3}})} \tag{11}$$

$$P_s = N\mu_1 \tag{12}$$

Case 5 : System $\langle 100 \rangle + \langle 111 \rangle$ and electric field along $\langle 110 \rangle$ direction : Using Table 5 and eqn. (4) we have expression for polarization given as

$$P = N \; \frac{2\left\{(\mu_1/\sqrt{2}) (e^{x_1/\sqrt{2}} - e^{-x_1/2})\right\} + 2\left\{(2\mu_2/\sqrt{6}) (e^{2x_2/\sqrt{6}} - e^{-2x_2/\sqrt{6}})\right\}}{2 + 2(e^{x_1/\sqrt{2}} + e^{-x_1/\sqrt{2}}) + 4 + 2(e^{2x_2/\sqrt{6}} + e^{-2x_2/\sqrt{6}})}$$

$$P = N \; \frac{(\mu_1/\sqrt{2}) (e^{x_1/\sqrt{2}} - e^{-x_1/\sqrt{2}}) + (\sqrt{2}/3) \,\mu_2 (e^{2x_2/\sqrt{6}} - e^{-2x_2/\sqrt{6}})}{3 + e^{x_1/\sqrt{2}} + e^{-x_1/\sqrt{2}} + e^{2x_2/\sqrt{6}} + e^{-x_2/\sqrt{6}}} \tag{13}$$

$$P_s = N\mu/2 \tag{14}$$

Case 6 : System $\langle 100 \rangle + \langle 111 \rangle$ and electric field along $\langle 111 \rangle$ direction : Using Table 6 and eqn. (4) we have expression for polarization given as

$$P = N \frac{3\left\{(\mu_1/\sqrt{3})(e^{x_1/\sqrt{3}} - e^{-x_1/\sqrt{3}})\right\} + \mu_2\left\{(e^{x_2} - e^{-x_2}) + (3/3)(e^{x_2/3} - e^{-x_2/3})\right\}}{3(e^{x_1/\sqrt{3}} + e^{-x_1/\sqrt{3}}) + e^{x_2} + e^{-x_2} + 3(e^{x_2/3} + e^{-x_2/3})}$$

$$P = N \frac{\sqrt{3}\,\mu_1(e^{x_1/\sqrt{3}} - e^{-x_1/\sqrt{3}}) + \mu_2(e^{x_2} - e^{-x_2} + e^{x_2/3} - e^{-x_2/3})}{3(e^{x_1/\sqrt{3}} + e^{-x_1/\sqrt{3}}) + e^{x_2} + e^{-x_2} + 3e(e^{x_2/3} + e^{-x_2/3})} \tag{15}$$

$$P_s = N\mu_2 \tag{16}$$

Now expressions for polarization for <100> and <100> + <111> model (present model) are listed in Table 7.

Results and Discussion

The expression for polarization for the <100> off-centred model for impurity is summarized in Table 7. The same table also lists the expressions for polarization for present model of simultaneous minima along the <100> and <111> directions. The off- centre displacement along the <100> and <111> directions, the saturation polarization for fields along the <100> and <111> directions should be equal (*cf.* Teble 7 for the case $\mu_1 = \mu_2$). The larger polarization for the <100> field in this case only indicates that the off-centre displacement of impurity of the <100> minima direction is larger than that in the <111> direction.

References

1. Devonshire, A.F. (1936) *Proc. R. Soc. London, Ser.* **153** (A) : 601.

2. Lawless, W.N. (1967) *J. Phys. Chem. Solids* **28** : 1755.

3. Seward, W.D. & Narayanmurthi, V. (1966) *Phys. Rev.* **148** : 463.

4. Flygare, W.H. (1963) *J. Chem. Phys.* **39** : 2263.

5. Mann, D.E., Acquista, N. & White, D. (1966) *J. Chem. Phys.* **44** : 3453.

6. Mitra, D.N., Agrawal, V.K. & Pandey G.K. (190) *Solid State Commun.* **8** : 1645.

7. Beyeler, H.U. (1972) *Phys. Status Solidi* **53**(B) : 419.

8. Pandey, G.K., Pandey, K.L., Massey, M. & Raj Kumar (1986) *Phys. Rev.* **34**(B) : 1277.

9. Gomez, M., Bowen, S.P. & Krumhansl, Z.A. (1967) *Phys. Rev.* **153** : 1009.

10. Dreyfus, R.W. (1968) *J. Phys. Chem. Solids* **29** : 1941.

11. Harrison, J.P., Peressini, P.P. & Pohl, R.O. (1968) *Phys. Rev.* **167** : 856.

12. Luty, F. (1974) *Phys. Rev.* **10**(B) : 3677.

13. Beyeler, H.U. (1975) *Phys. Rev.* **11**(B) : 3078.

14. Quingley, R.J. & Das, T.P. (1973) *Phys. Rev.* **7**(B) : 4004.

15. Rollefson, R.J. (1972) *Phys. Rev.* **%**(B) : 3235.

16. Rollefson, R.J (1973) *Phys. Rev.* **7**(B) : 4006.

Liquid crystalline behaviour of alkoxybenzoic acids : A theoretical study

S.N. TIWARI and NITISH K. SANYAL*

Department of Physics, D.D.U. Gorakhpur University, Gorakhpur - 273 009, India

*Vice Chancellor, U.P. Rajarshi Tandon Open University, Allahabad - 211 001, India

Abstract

Molecular interactions between a pair of molecules of the homologous series para-n-alkoxybenzoic acid have been evaluated using quantum mechanical methods. Both, stacking as well as in-plane interacting configurations have been taken into account. Results obtained have been used to discuss the molecular forces responsible for the mesogenic behaviour of the systems. An attempt has been made to explain mesogenic and non-mesogenic characters exhibited by different members of the same homologous series in terms of the intermolecular interactions.

(**Keywords** : liquid crystals/molecular interactions/CNDO/mesogen/alkoxybenzoic acids).

Introduction

Molecular ordering in mesomorphic substances has been receiving attention for quite sometime[1]. A number of theoretical models to explain the liquid crystallinity have been reported from time to time[2-5]. These models, largely concerned with nematogenic materials, attempt to explain the observed orientational order for such systems. The molecular field approach[4] presently deemed to be the most popular and successful one is based on the following[6]:

(i) The assumption of an induced-dipole induced-dipole interaction between molecules of the liquids as the sole cause of transition,

(ii) The assumption that the probability of any configuration of centres of mass is not affected by the interaction between different molecular orientations, and

(iii) The molecular field approximation to treat the resulting problem of interacting orientations.

Later modifications have included parameters representing repulsive or polarization potential which were essentially qualitative in nature[7,8]. Commonly, a simple anisotropic pair potential, $U(r_{12}, \theta_{12}) = - U(r_{12}) \, P_2(\cos \theta_{12})$ is used; where U is a scalar potential, $P_2(\cos \theta_{12})$ is a second Legendre polynomial, r_{12} and θ_{12} are the separation and angle between the molecules 1 and 2 respecively[9]. Also, the cylindrical symmetry of the rod like molecules is assumed together with the equivalence of θ and $(\pi - \theta)$. These assumptions based on some experimental evidences, help to reduce computational complexities.

The peculiar changes–characteristics of mesomorphic behaviour which occur at phase transitions, are primarily governed by the intermolecular interactions acting between sides, planes and ends of a pair of molecules[1]. In view of the key role of molecular interactions in mesogenic compounds, semi-empirical calculations have been emphasized and carried out by several workers with an aim to explain liquid crystallinity[10-12]. Tokita et al.[12] used Lennard-Jones potential to evaluate intermolecular interactions between a pair of pure nematogens and attempted to correlate their results with those of the molecular field theory[5]. However, it has been observed that '6-exp' type of potential functions are found to be more effective in explaining the molecular packing instead of Lennard-Jones potentials[13]. It is therefore, considered worthwhile to examine the anisotropy of interactions between a pair of mesomorphic molecules. In our earlier communications, using Rayleigh-Schrodinger perturbation theory modified with multicentered–multipole expansion method, intermolecular interaction energy has been evaluated in case of several mesogens[14-18]. Also, an attempt has been made to correlate the mesogenic properties with molecular interactions. In continuation of our earlier studies on thermotropic liquid crystals[14-18], interaction energy studies between a molecular pair of the following systems have been reported in this paper:

 (i) para-n-methoxybenzoic acid (PMB)

 (ii) para-n-propoxybenzoic acid (PPB)

 (iii) para-n-octyloxybenzoic acid (POB)

 The general feature of all these molecules is that they possess a polarizable aromatic ring associated with two highly electronegative atoms (oxygens of carboxylic group) at one end and the alkoxychain at the other. These acid molecules are capable of forming head to head pairs due to the hydrogen bonds between the –COOH end groups of the molecules[19]. An examination of the thermodynamic data for the homologous series indicates that PMB is a pure liquid which gives a clear melt at 184°C for C $\longrightarrow$ I transition[20]. PPB transforms to a nematic mesophase exhibiting C $\xrightarrow{\text{121°C}}$ C,   C $\xrightarrow{\text{146.5°C}}$ N,   and

$N \xrightarrow{153.5°C} I$ transitions while POB shows both, nematic and smectic mesophases at different

temperatues as under :

$$C \xrightarrow{75°C} C, \quad C \xrightarrow{101°C} S, \quad S \xrightarrow{108°C} N, \quad N \xrightarrow{146°C} I$$
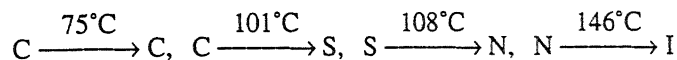
Theoretical Method

The choice of an adequate method for evaluation of interactions between a molecular pair seems to be important. The total intermolecular interaction energy (E_{tot}), neglecting the resonance and magnetic interactions, between a pair of molecules can be expressed as:

$$E_{tot} = E_{el} + E_{pol} + E_{disp} + E_{rep} \tag{1}$$

where E_{el}, E_{pol}, E_{disp} and E_{rep} represent electrostatic, polarization, dispersion and repulsion components respectively.

According to Rayleigh-Schrodinger perturbation treatment for long-range interactions, the electrostatic term is obtained as a first order perturbation energy while the induction and dispersion energy components are obtained as the second order perturbation terms[21-22]. Repulsion energy is calculated separately either from the repulsive part of Lennard-Jones or Buckingham type of potentials or from an optimized potential function including the repulsive and attractive (dispersion) terms[23].

The aforesaid method has difficulties because the complete process of evaluation of energy has to be carried out separately for each pair of molecules while a more practical method would be to develop certain parameters in terms of individual molecular properties such as multipole moments, polarizability etc. which may reduce the conceptual complexities and computational complications. In literature, a number of methods based on R-S treatment are available on these lines[24]. Earlier workers employed one centre expansion of the multipole moments to evaluate electrostatic energy[25-26]. This method was found to be suitable for smaller molecules while for larger systems, however, intermolecular separation can no longer be treated very large as compared to the molecular dimensions. Also R-S treatment has some inherent inadequacies at short ranges as discussed by Claverie[27].

An alternative approach, commonly referred to as multicentred- multipole expansion method appears to be more appropriate for larger molecular systems[28]. In this approach, instead of taking the centre of mass of the whole molecule as the centre of expansion,

multipoles corresponding to each atomic centre of the molecule, are evaluated using all valence molecular orbital methods such as SCFσ + Huckel π, Del Reσ + Huckelπ, CNDO, EHT, IEHT etc. However, CNDO/2 method is preferred because of its simplicity and capability to predict correct dipole moment etc[29]. Usually, the evaluation of atomic net charges and dipoles is sufficient to treat the interaction problem with a reasonable accuracy. A number of successful applications to biomolecular interactions have placed the method on a strong ground to account for the short and intermediate range interactions of large molecules[30-36]. In the present computation, the method developed by Claverie has been followed.

Electrostatic energy : According to the multicentred-multipole expansion, the electrostatic term is expressed as

$$E_{el} = E_{qq} + E_{qmi} + E_{mimi} + \ldots \ldots \qquad (2)$$

where E_{qq}, E_{qmi} and E_{mimi} etc. represent monopole-monopole, monopole-dipole, dipole-dipole and other higher order interaction energy terms respectively. The electrostatic component arising due to higher order multipole moments also exist but only an evaluation of electrostatic energy upto the first three terms has been found suitable for most of the cases[37].

Again, monopole-monopole energy is given as :

$$E_{qq} = C \sum_{i,j} \frac{q_i \, q_j}{r_{ij}} \qquad (3)$$

where q_i, q_j are monopoles at each of the atomic centres of the interacting molecules while r_{ij} is the inter-atomic distance. The constant, C, is a conversion factor, approximately equal to 332, which expresses the energy in kilocalories per mole of the dimer.

The monopole-dipole energy is expressed as :

$$E_{qmi} = C \sum_{i,j} q_i \, \vec{\mu_j} \cdot \frac{\vec{r}}{r^3} \qquad (4)$$

while dipole-dipole term is given by

$$E_{mimi} = C \sum_{i,j} \frac{1}{r^3} \left[\vec{\mu_i} . \vec{\mu_j} - 3 \left(\vec{\mu_i} . \frac{\vec{r}}{r} \right) \left(\vec{\mu_j} . \frac{\vec{r}}{r} \right) \right] \qquad (5)$$

where μ_i, μ_j represent the atomic dipoles, the subscript of r has been removed without any change in its meaning and other notations have the same meaning as in eqn. (3).

Polarization energy : The polarization energy of a molecule, say (s), is obtained as a sum of the polarization energies for the various bonds

$$E_{pol}^{(s)} = C\,(-1/2)\,\sum_u^{(s)}\varepsilon_u^{[s]}\,A_u^{(s)}\,\varepsilon_u^{[s]} \qquad (6)$$

where $\qquad \varepsilon_u^{[s]} = \sum_{t \neq s}\,\sum_\lambda{}'\,q_\lambda^{(t)}\,\vec{R}_{\lambda u}\,/\,R_{\lambda u}^3 \qquad (7)$

is the electric field created at bond u by all the surrounding molecules and A_u is the polarizabilty tensor of this bond. $\vec{R}_{\lambda u}$ is the vector joining the atom λ in molecule (t) to the 'centre of polarizable charge' on the bond u of molecule (s).

Dispersion and repulsion energy : Dispersion and repulsion terms are calculated together using Kitaigorodskii[38-39] type of formulae

$$E_{disp} + E_{rep} = \sum_\lambda^{(1)}\,\sum_v^{(2)}\,E\,(\lambda, v) \qquad (8)$$

here $\qquad E\,(\lambda, v) = K_\lambda\,K_v\,(-A/z^6 + Be^{-\gamma z})$

and $\qquad z = R_{\lambda v}/R_{\lambda v}^0\,;\; R_{\lambda v}^0 = \sqrt{(2R_\lambda^w)\,(2R_v^w)} \qquad (9)$

Here R_λ^w and R_v^w are van der Waal's radii of atoms λ and v respectively. The parameters A, B and γ do not depend on the atomic species, but $R^\circ{}_{\lambda v}$ and the factors K_λ and K_v depend on the atomic species involved. The recent values of these parameters have been taken from literature[40-41].

The molecular geometry of PMB has been taken from literature[42]. PPB and POB have been constructed using crystallographic data together with the standard values of bond lengths and bond angles. Complete neglect of differential overlap method, (CNDO/2), has been employed to compute the net atomic charge and dipoles on the various atomic centres of the molecules[43].

The energy minimization has been carried out for both stacked and in-plane interactions separately in all the systems under study. One of the interacting molecules is kept fixed
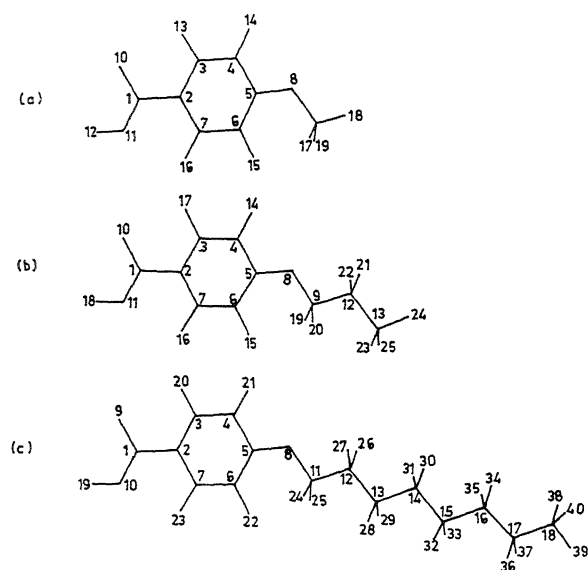
Fig. 1 – Molecular geometries of systems studied alongwith various atomic index numbers. (a) p-n-methoxybenzoic acid (PMB), (b) p-n- propoxybenzoic acid (PPB), (c) p-n-octyloxybenzoic acid (POB).
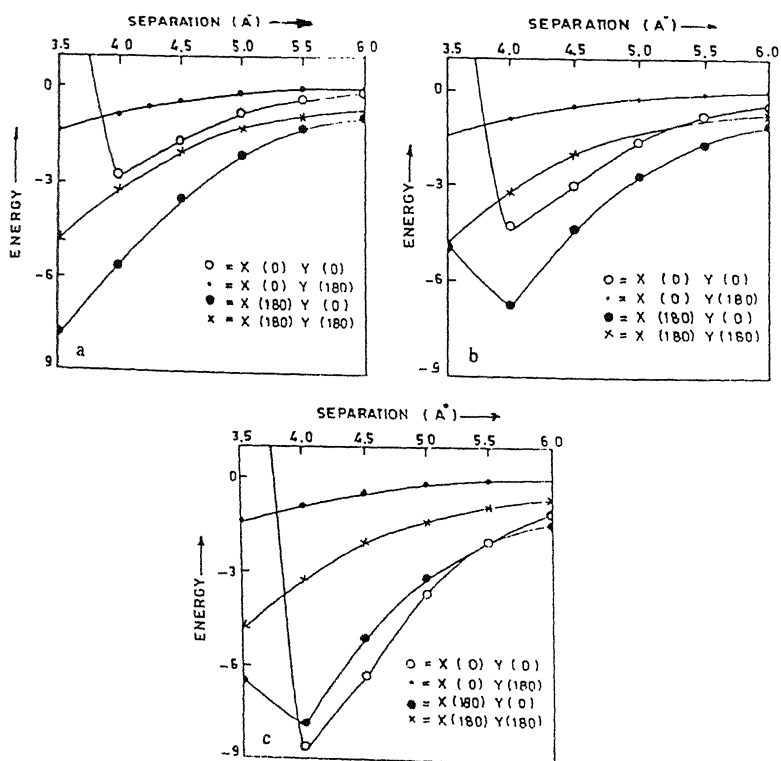

Fig. 2 – Variation of stacking energy with respect to interplanar separation. Energy is expressed in kcal/mole of dimer. (a) p-n- methoxybenzoic acid, (b) p-n-propoxybenzoic acid, (c) p-n- octyloxybenzoic acid.

iroughout the process while variation in both, angular and lateral positions are given in ie other molecule in all respects relative to the fixed one. Accuracies upto 0.1 A° during liding (or translation) and 1° in rotation, have been achieved. All the computations were arried out on CDC 'Cyber -- 170' computer at Tata Institute of Fundamental Research, Mumbai.

Results and Discussion

Molecular geometries of PMB, PPB and POB alongwith their atomic index numbers are shown in Fig. 1 while the net atomic charge and dipole moment components corresponding to each atomic centre are listed in Tables (1-3) respectively for PMB, PPB and POB molecules. The total energy, binding energy, total dipole moment and its components are given in Table 4 for all the homologues under study.

As is evident from Tables (1-3), the oxygen atoms of carboxylic groups O_{10} of methoxy and propoxybenzoic acids and O_9 of octyloxybenzoic acid molecule have a constant value for the net atomic charge (-0.35 e) while the other oxygen atom O_{11} of PMB and PPB and O_{10} of POB also have a constant charge equal to -0.225 e. Since the carboxylic oxygen atoms are associated with greater negative charges and attached to one end of the p-n-alkoxybenzoic acid molecules, they are always capable of forming hydrogen bonded dimers whenever any proton is available to them – a fact observed experimentally[42]. Also, the total dipole moment for benzoic acid molecules (Table 4) shows a fairly constant value while the magnitude of the total energy has the following order :

PMB < PPB < POB
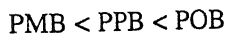
This indicates that addition of methylene group confers additional stability to the packing of the members of this homologous series. The interaction energy between a pair of molecules has been analysed in terms of several parameters as described below.

Separation : This has been carried out by keeping the long molecular axes of the interacting molecules parallel to each other. In this case, the coordinate axes (X, Y, Z) are defined such that X-axis is directed along the long molecular axis with Y-axis being perpendicular to it and lying in the molecular plane while Z-axis is perpendicular to the plane of the molecule and passes through the centre of gravity of the molecule, which is chosen as the origin. To obtain the most stable configuration (maximum attraction condition), the molecules are considered either in (a) stacked or (b) in-plane interacting configurations. In the case of stacking interactions, the interplanar separation between a pair of molecules is varied from 3.5 A° onwards at an interval of 0.5 A° and at each point

Table 1 – Molecular charge distribution of p-n-methoxybenzoic acid.

Atom No.	Symbol	Charge (e.u.)*	Atomic dipole components (Debye)		
			X	Y	Z
1	C	0.392	− 0.217	− 0.221	− 0.014
2	C	− 0.063	0.070	− 0.034	− 0.049
3	C	0.055	0.060	− 0.146	− 0.001
4	C	− 0.061	− 0.084	− 0.170	0.005
5	C	0.210	0.232	0.033	− 0.027
6	C	− 0.068	− 0.057	0.157	0.016
7	C	0.047	0.080	0.121	− 0.001
8	O	− 0.210	− 0.626	− 1.210	− 0.069
9	C	0.122	− 0.198	0.244	0.034
10	O	− 0.351	0.644	− 1.209	0.029
11	O	− 0.255	−0.555	1.157	0.087
12	H	0.167	0.000	0.000	0.000
13	H	0.004	0.000	0.000	0.000
14	H	0.015	0.000	0.000	0.000
15	H	0.006	0.000	0.000	0.000
16	H	− 0.001	0.000	0.000	0.000
17	H	− 0.006	0.000	0.000	0.000
18	H	0.003	0.000	0.000	0.000
19	H	− 0.006	0.000	0.000	0.000

*e.u. = electron unit

Table 2 – Molecular charge distribution of p-n-propoxybenzoic acid.

Atom No.	Symbol	Charge (e.u.)*	Atomic dipole components (Debye)		
			X	Y	Z
1	C	0.393	− 0.220	− 0.220	− 0.014
2	C	− 0.063	0.068	− 0.034	− 0.049
3	C	0.055	0.057	− 0.144	− 0.001
4	C	− 0.063	− 0.087	− 0.165	0.003
5	C	0.207	0.211	− 0.036	− 0.023
6	C	− 0.070	− 0.060	0.153	0.017
7	C	0.048	0.078	0.120	− 0.001
8	O	− 0.255	− 0.631	− 1.187	0.002
9	C	0.155	− 0.076	0.233	0.006
10	O	− 0.353	0.643	− 1.209	0.029
11	O	− 0.255	− 0.556	1.157	0.087
12	C	0.005	− 0.039	0.012	− 0.140
13	C	− 0.005	− 0.131	0.141	− 0.005
14	H	0.013	0.000	0.000	0.000
15	H	0.004	0.000	0.000	0.000
16	H	− 0.002	0.000	0.000	0.000
17	H	0.003	0.000	0.000	0.000
18	H	0.166	0.000	0.000	0.000
19	H	− 0.016	0.000	0.000	0.000
20	H	− 0.017	0.000	0.000	0.000
21	H	0.007	0.000	0.000	0.000
22	H	0.005	0.000	0.000	0.000
23	H	0.003	0.000	0.000	0.000
24	H	0.001	0.000	0.000	0.000
25	H	0.003	0.000	0.000	0.000

*e.u. = electron unit

Table 3 – Molecular charge distribution of p-n- octyloxybenzoic acid.

Atom No.	Symbol	Charge	Atomic dipole componnts (Debye)		
		(e.u.)*	X	Y	Z
1	C	0.393	– 0.220	– 0.221	– 0.014
2	C	– 0.063	0.067	– 0.034	– 0.049
3	C	0.055	0.057	– 0.144	– 0.001
4	C	– 0.063	– 0.087	– 0.164	0.005
5	C	0.207	0.209	0.036	– 0.025
6	C	– 0.070	– 0.060	0.152	0.016
7	C	0.048	0.077	0.120	– 0.001
8	O	– 0.226	– 0.637	– 1.182	– 0.059
9	O	– 0.353	0.643	– 1.209	0.029
10	O	– 0.255	– 0.556	1.157	0.087
11	C	0.153	– 0.086	0.229	0.022
12	C	– 0.001	– 0.044	– 0.127	0.005
13	C	0.022	0.003	0.115	– 0.017
14	C	0.017	– 0.025	– 0.079	0.021
15	C	0.018	0.030	0.083	– 0.022
16	C	0.022	– 0.010	– 0.080	0.016
17	C	0.025	0.035	0.084	– 0.010
18	C	– 0.009	– 0.155	– 0.045	0.007
19	H	0.166	0.000	0.000	0.000
20	H	0.002	0.000	0.000	0.000
21	H	0.013	0.000	0.000	0.000
22	H	0.004	0.000	0.000	0.000
23	H	– 0.002	0.000	0.000	0.000
24	H	– 0.017	0.000	0.000	0.000
25	H	– 0.017	0.000	0.000	0.000
26	H	0.007	0.000	0.000	0.000
27	H	0.004	0.000	0.000	0.000
28	H	– 0.007	0.000	0.000	0.000
29	H	– 0.006	0.000	0.000	0.000
30	H	– 0.007	0.000	0.000	0.000
31	H	– 0.006	0.000	0.000	0.000
32	H	– 0.008	0.000	0.000	0.000
33	H	– 0.009	0.000	0.000	0.000
34	H	– 0.009	0.000	0.000	0.000
35	H	– 0.009	0.000	0.000	0.000
36	H	– 0.009	0.000	0.000	0.000
37	H	– 0.010	0.000	0.000	0.000
38	H	0.001	0.000	0.000	0.000
39	H	– 0.003	0.000	0.000	0.000
40	H	0.001	0.000	0.000	0.000

*e.u. = electron unit
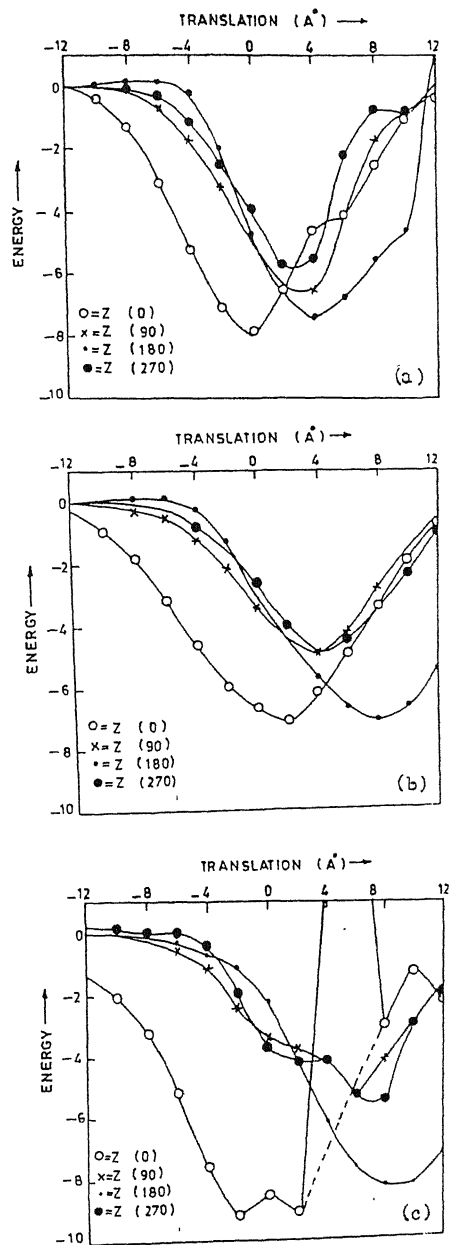
Fig. 3 – Variation of total stacking energy with respect to sliding (translation) along the long molecular axis
(X). Energy is expressed in kcal/mole. (a) p-n-methoxybenzoic acid, (b) p-n- propoxybenzoic acid, (c)
p-n-octyloxybenzoic acid.

64
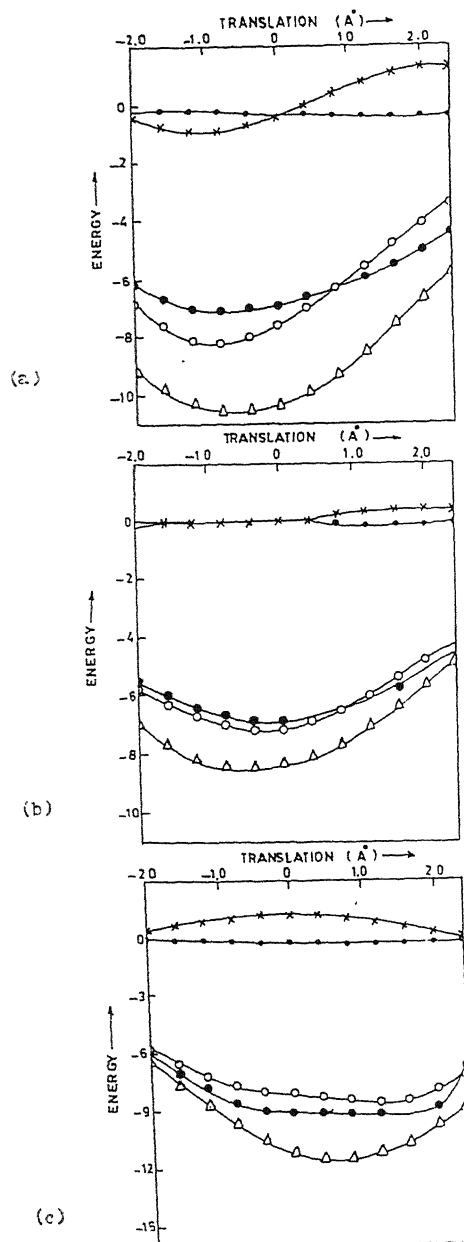
Fig. 4 – Variation of stacking energy components with respect to sliding along the long molecular axis (X). Energy is expressed in kcal/mole. Notations are same as mentioned in Fig. 4(a). (a) p-n- methoxybenzoic acid, (b) p-n-propoxybenzoic acid, (c) p-n- octyloxybenzoic acid.

Fig. 5 – Variation of stacking energy components with respect to sliding (translation) along an axis perpendicular to the long molecular axis(Y). Energy is expressed in kcal/mole. Notations are same as mentioned in Fig. 4(a). (a) p-n-methoxybenzoic acid, (b) p-n-propoxybenzoic acid, (c) p-n-octyloxybenzoic acid.

Table 4 – Total energy*, binding energy**, total dipole moment and its components for systems studied.

Molecule	Total energy	Binding energy	Dipole moment (Debye)			
	(atomic unit)	(atomic unit)	μ_X	μ_Y	μ_Z	Total (μ)
PMB	– 118.13	– 9.46	0.12	– 2.22	0.03	2.23
PPB	– 135.53	– 11.97	0.27	– 2.23	0.09	2.25
POB	– 178.99	– 18.21	0.30	– 2.27	0.00	2.29

* Total energy corresponds to the sum of atomic as well as electronic energies of all the constituents of the molecule in the equilibrium geometry.
** Binding energy of a molecule is the difference between the total energy of the equilibrium molecular geometry and the sum of the atomic energies of the constituent atoms.

Table 5 – Interaction energy components for stacking and in- plane minimum energy configurations. Energy is expressed in kcal/mole.

Interaction energy terms	Stacking energy			In-plane energy		
	PMB	PPB	POB	PMB	PPB	POB
E_{qq}	– 0.02	0.21	0.64	– 0.15	– 0.22	– 0.19
E_{qmi}	– 0.01	0.31	0.82	– 0.24	– 0.45	– 0.41
E_{mimi}	– 1.35	– 0.71	1.03	– 0.01	– 0.11	– 0.10
E_{el}	– 1.38	– 0.19	2.49	– 0.40	– 0.78	– 0.69
E_{pol}	– 0.35	– 0.42	– 0.43	– 0.34	– 0.26	– 0.30
E_{disp}	– 14.01	– 14.13	– 20.47	– 3.31	– 3.91	– 6.64
E_{rep}	6.99	5.96	7.17	1.28	1.92	3.01
E_{tot}	– 8.76	–8.78	– 11.24	– 2.77	– 3.03	– 4.62

energies are evaluated. All the possible stacked configurations have been examined by allowing rotations through 180° about the X-axis, Y-axis or both axes. The results obtained, have been graphically shown in Fig. 2 (a,b,c). It is clear from this figure that variations in the total stacking energy with respect to interplanar separation, are similar for all the cases corresponding to the condition when both the stacked molecules are lying overlapped exactly one above the other and the complexes are stablized at 4.0 A°.
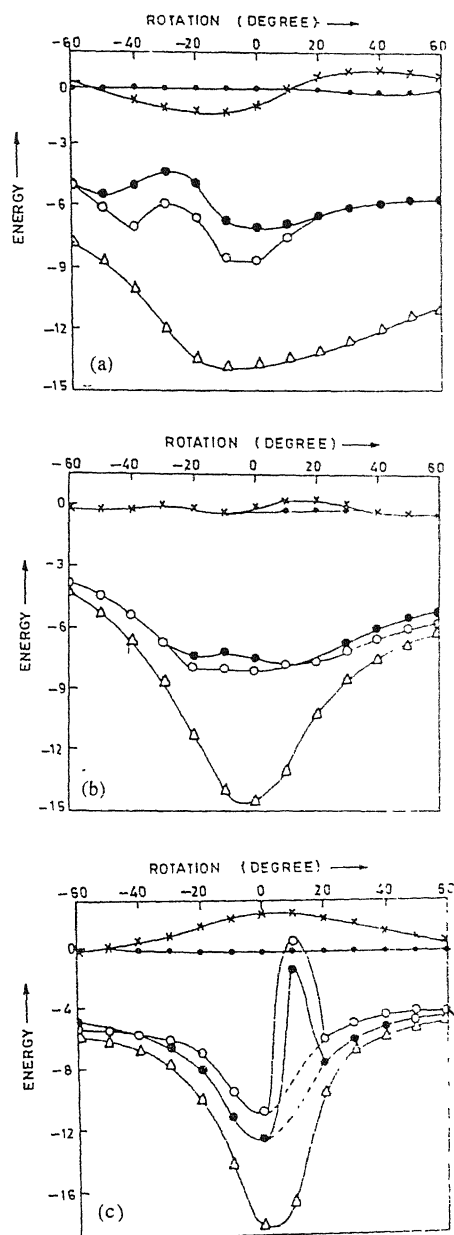
Fig. 6 – Variation of stacking energy with respect to rotational angle. Energy is r.... are same as mentioned in Fig. 4(a). (a) p-n-methoxybenzoic acid, (b) p... p-n-octyloxybenzoic acid.

Table 4 – Total energy*, binding energy**, total dipole moment and its components for systems studied.

Molecule	Total energy (atomic unit)	Binding energy (atomic unit)	Dipole moment (Debye)			
			μ_X	μ_Y	μ_Z	Total (μ)
PMB	– 118.13	– 9.46	0.12	– 2.22	0.03	2.23
PPB	– 135.53	– 11.97	0.27	– 2.23	0.09	2.25
POB	– 178.99	– 18.21	0.30	– 2.27	0.00	2.29

* Total energy corresponds to the sum of atomic as well as electronic energies of all the constituents of the molecule in the equilibrium geometry.
** Binding energy of a molecule is the difference between the total energy of the equilibrium molecular geometry and the sum of the atomic energies of the constituent atoms.

Table 5 – Interaction energy components for stacking and in- plane minimum energy configurations. Energy is expressed in kcal/mole.

Interaction energy terms	Stacking energy			In-plane energy		
	PMB	PPB	POB	PMB	PPB	POB
E_{ej}	– 0.02	0.21	0.64	– 0.15	– 0.22	– 0.19
E_{qmi}	– 0.01	0.31	0.82	– 0.24	– 0.45	– 0.41
E_{mimi}	– 1.35	– 0.71	1.03	– 0.01	– 0.11	– 0.10
$E_{e.}$	– 1.38	– 0.19	2.49	– 0.40	– 0.78	– 0.69
E_{i}	– 0.35	– 0.42	– 0.43	– 0.34	– 0.26	– 0.30
E_{disp}	– 14.01	– 14.13	– 20.47	– 3.31	– 3.91	– 6.64
E_{re}	6.99	5.96	7.17	1.28	1.92	3.01
E_{tot}	– 8.76	–8.78	– 11.24	– 2.77	– 3.03	– 4.62

energies are evaluated. All the possible stacked configurations have been examined by allowing rotations through 180° about the X-axis, Y-axis or both axes. The results obtained, have been graphically shown in Fig. 2 (a,b,c). It is clear from this figure that variations in the total stacking energy with respect to interplanar separation, are similar for all the cases corresponding to the condition when both the stacked molecules are lying overlapped exactly one above the other and the complexes are stablized at 4.0 A°.

Fig. 6 – Variation of stacking energy with respect to rotational angle. Energy is expressed in kcal/mole. Notati are same as mentioned in Fig. 4(a). (a) p-n-methoxybenzoic acid, (b) p-n- propoxybenzoic acid, p-n-octyloxybenzoic acid.

However, the anisoptropic nature of pair interactions is reflected in the stacked complexes for PMB and PPB possessing maximum attraction at 3.5 and 4.0 A° respectively with a rotation of 180° about the X-axis while the minimum energy stacked complex for POB corresponds to the overlapped structure at a separation of 4.0 A° (Fig. 2). Rotation about Y-axis by 180° shows minimum attraction and that about both the axes gives intermediate attraction showing a minimum at 3.5 A° in all the cases. This implies that in closed molecular packing, PMB and PPB are stacked such that in a molecular pair, one of the molecules is rotated by 180° about its own long molecular axis while no such rotation about any axis is needed for stablizing the molecular pair of POB molecules. It may be observed here that the effective range of the stacking interactions is of the order of 6.0 A° – interplanar separation of the dimer (Fig. 2).

Sliding : The translational freedom of one molecule over the other, is examined by sliding one molecule with respect to the other along both X and Y axes corresponding to the lower energy stacked molecular pair obtained from Fig. 2. For X-sliding (translation), four preselected rotations about the Z-axis viz. Z(0°), Z(90°), Z(180°), Z(270°) were introduced with a view to reach the extreme conditions and corresponding to each rotation, sliding energy is calculated in the range of ± 12.0 A° at an interval of 2.0 A°. The results have been plotted in Fig. 3 (a,b,c). As is evident from this figure, the sliding energy corresponding to Z(90°) and Z(270°) has relatively lower value. This is obvious because of the least molecular overlapping in these cases. A sharp and deep minimum is located in the case of PMB (Fig. 3a) while relatively flat and wider regions are observed for the other two molecules. It is interesting to note that the variation of sliding energy corresponding to each rotation is similar in the case of PMB. The maximum energy difference lies within 2 kcal/mole of dimer which indicates that at increased thermal agitations, the probabilities of resting in parallel and perpendicular stacking patterns become almost equivalent. This seems to be the reason why PMB directly goes to an isotropic melt state which represents a completely disorganised three dimensional structure.

In the case of PPB, the two curves corresponding to Z(0°) and Z(180°) rotations show flat regions. For Z(0°), the region starts from + 2.0 to – 4.0 A°, a span of 6.0 A° in which energy variations are minor (approximately 1 kcal/mole) while a similar flat region in the curve corresponding to Z(180°) is noticed between +4.0 to 11.0 A°, a span of 7.0 A°. These flat regions indicate the existence of translational freedom of the molecules along their long molecular axes. The energy for Z(180°) is slightly lower than that of Z(0°) and as such, has been undertaken for further study. In the case of POB, flat regions are obtained for both Z(0°) and Z(180°), but the energy corresponding to Z(180°) is higher as compared to Z(0°) and, hence, the minimum located by Z(0°) curve, is preferred for further calculations. Rapid increase in energy, observed between 3.0 and 8.0A° appears due to the violation of
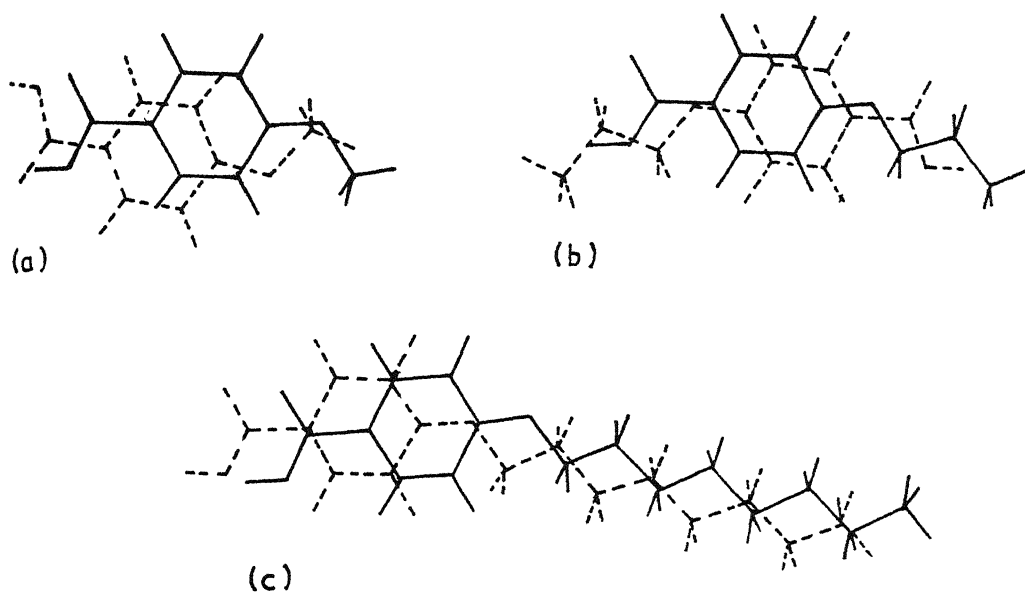
Fig. 7 – Minimum energy stacked complexes for (a) PMB, (b) PPB and (c) POB molecules with interplanar separation (a) 3.3A°, (b) 3.6A° and (c) 3.7 A° respectively. Energy details are given in Table 5.
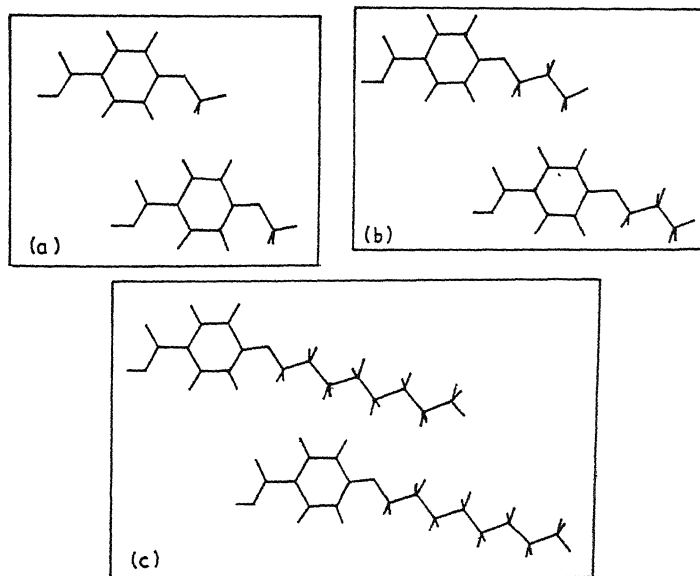

Fig. 8 – Minimum energy in-plane configurations for (a) PMB, (b) PPB and (c) POB molecules with intermolecular separation (a) 6.1A°, (b) 6.5A° and (c) 7.0 A° respectively. Energy details are given in Table 5.

van der Waal contact distances for C(H)—C(H) between the methyl groups. It may be noted that the stacked pair energy is minimised at 4.0 A° (Fig. 2c) while C(H)—C(H) contact distance is 4.20 A°. Hence, by slightly increasing the interplanar separation, one may sufficiently reduce such repulsive forces.

The variation of different interaction energy components corresponding to the rotational minima obtained from Fig. 3 (a,b,c), has been shown in Fig. 4 (a,b,c). As is evident from this figure, polarization component is weak while electrostatic energy curve assumes both, attractive and repulsive nature but is insignificant. The only dominant term is due to 'short range' dispersion and repulsion components. The repulsion energy term has not been plotted explicitly as it can be easily obtained from Kitaigorodskii (dispersion + repulsion) and dispersion energy curves. The repulsion region, noticed for POB, is also supported by Kitaigorodskii curve implying that though dispersion energy is highly attractive but the sudden increase in the repulsive energy results in the repulsive nature of the total energy. The dominant role of dispersion forces (induced dipole-induced dipole) in stabilizing the packing of mesogens, has been also recognized by several other workers[12,44,45].

The variation of intermolecular interaction energy components for sliding along Y-axis, has been shown in Fig. 5 (a,b,c) respectively for PMB,PPB and POB molecules. It is obvious from this figure that only for translations within the range of ± 2.0 A°, energy largely changes in case of PMB. In other words, a change of approximately 4.5 kilocal/mole of dimer is observed for PMB while PPB and POB exhibit relatively smaller changes in the energy (approximately 2 kcal/mole). However, this change in energy is higher as compared to sliding along X-axis as shown in Fig. 3 (a,b,c) implying that there is a lesser possibility of sliding of the stacked molecules along an axis perpendicular to the long molecular axis in the molecular plane. Gross similarity exist in the total and Kitaigorodskii (dispersion + repulsion) energy curves.

Rotation : The variation of interaction energy components with respect to rotation corresponding to the minimum energy points obtained from Fig. 5 (a,b,c) has been plotted in Fig. 6 (a,b,c) respectively for PMB, PPB and POB molecules. Both, clockwise and anticlockwise rotations in the range of ± 60°, has been given with an aim to examine the angular dependence of stacking energy. It is interesting to note from Fig. 6(c) that maximum selectivity is obtained for POB while PMB shows maximum orientational freedom. The orientational freedom of PPB is intermediate with minor changes in energy (approximately 1 kcal/mole) within range of ± 20°. Also the minimum for POB corresponds to −10.0 kcal/mole which is largest in magnitude as compared to PMB or PPB molecules. This indicates that the tendency of forming aligned structure is maximum in the case of POB which supports the smectic character of system at lower temperatures in the mesomorphic range.

The minimum energy configurations were subjected to further refined calculations to achieve the final lowest energy configurations. The minimum energy stacked complexes thus obtained, have been shown in Fig. 7 (a,b,c) while the energy distribution has been listed in Table 5. It is observed that two molecules of PMB are stabilized at 3.30 A° such that one of them has been rotated by 180° both about X and Z-axes. It is interesting to note that PMB and PPB both have the same order of energy values (nearly 9.0 kcal/mole) but differ in their respective stacking patterns. Though the stacking pattern of POB molecules is similar to PMB, there is an increase in interplanar separation (3.70 A°) with a lowering in the stacking energy (–11.24 kcal/mole for POB) which is probably due to the long alkoxychain attached to POB. The minimum energy configurations obtained from in-plane interactions, are shown in Fig. 8(a,b,c). It is significant to note that all the homologues under study exhibit similar in-plane minimum energy configurations. The in-plane energy for PMB and PPB are nearly the same – 3.0 kcl/mole while for POB the energy corresponds to – 4.62 kcal/mole. This implies that by increasing the alkoxy chain, in-plane attractions are largely increased as compared to the stacking which is in accordance with the experimental observations and likely to favour the smectic behaviour of the compound[1].

Conclusion

Computational results based on the consideration of actual molecular shape and composition indicate that the packing energy of the members of p-n-alkoxybenzoic acid series is in the following order :

POB > PPB > PMB
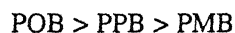
This shows that the stability of molecular packing increases with the addition of methylene group in the alkoxychain. The dominant forces between the mesogenic molecules are essentially of dispersion (induced dipole-induced-dipole) type which is in agreement with the basic assumption of the molecular field theory. Further, the analysis of energy variation with respect to orientation and sliding is helpful in discriminating mesogenic and non-mesogenic molecules. These studies may also be useful in characterizing smectic and nematic properties of molecules.

Acknowledgements

References

1. Gray, G.W. (1962) *Molecular Structure and Properties of Liquid Crystals*, Academic Press, London.

2. Onsager, L. (1949) *Ann. N.Y. Acad. Sci.*. **51** : 627.

3. Flory, P.J. (1956) *Proc. R. Soc. London* A234 : 73.

4. Maier, W. & Saupe, A. (1958) *Z. Naturf.* 13A : 564; (1959) *Z. Naturf.* 14A : 882; (1960) *Z. Naturf.* 15A : 287.

5. Chandrasekhar, S. (1977) *Liquid Crystals*, Cambridge University Press, England.

6. Schultz, T.D. (1972) *Liquid Crystals*, Vol. 3(1), eds., Brown, G.H. & Labes, M.M., Gordon and Breach Sci. Publ., New York, p. 263.

7. Chandrashekhar, S. & Madhusudana, N.V. (1970) *Mol. Cryst. Liq. Cryst.* **10** : 151.

8. Chandrashekhar, S. & Madhusudana, N.V. (1971) *Acta Cryst.* A27 : 303.

9. de Gennes, P.G. (1974) *The Physics of Liquid Crystals*, Clarendon Press, London.

10. Cotrait, M., Marsau, P., Pesques, M. & Volphilhac, V. (1982) *J. Physique* **43** : 355.

11. Berges, J. & Perrin, H. (1984) *Mol. Cryst. Liq. Cryst.* **113** : 269.

12. Tokita, K., Fujimura, K., Kondo, S. & Takeda, M. (1981) *Mol. Cryst. Liq. Cryst. Lett.* **64** : 171.

13. Pawley, G.S. (1987) *Phys. Stat.Sol.* **20** : 347.

14. Sanyal, N.K., Roychoudhury, M., Tiwari, S.N. & Shukla, S.R. (1985) *Mol. Cryst. Liq. Cryst.* **128** : 211.

15. Sanyal, N.K., Tiwari, S.N. & Roychoudhury, M. (1986) *Mol. Cryst. Liq. Cryst.* **132** : 81; **140** : 179.

16. Tiwari, S.N., Roychoudhury, M. & Sanyal, N.K. (1987) *Proc. Second Asia Pacific Physics Conference*, Vol. 2, ed. Chandrasekhar, S., World Sci. Publ. Comp., Singapore, p. 1081.

17. Tiwari, S.N., Roychoudhury, M. & Sanyal, N.K. (1991) *Mol. Cryst. Liq. Cryst.* **204** : 111.

18. Tiwari, S.N. & Sanyal, N.K. (1999) *Condensed Matter Physics*, eds., Agrawal, B.K. & Prakash, H., Narosa Publishing House, New Delhi, p. 178.

19. Petrov, M. & Durand, J. (1996) *J. Physique II* **6** : 1259.

20. Barrall, E.M. & Johnson, J.F. (1974) *Liquid Crystals and Plastic Crystals*, Vol. 2, eds., Gray, G.W. & Winsor, P.A., Ellis Harwood, Chichester, p. 254.

21. Claverie, P. (1976) *Localization and Delocalization in Quantum Chemistry*, Vol. 2, eds., Chalvet, O., Dandel, R., Dinner, S. & Malriev, J.P., D. Reidel Publ. Comp., Dordrecht-Holand, p. 127.

22. Buckingham, A.D. (1978) *Intermolecular Interactions : From Diatomics to Biopolymers*, ed., Pullman, B., John Wiley, New York, p. 1.

23. Ornstein, R.L., Rein, R., Breen, D.L. & MacElroy, D. (1978) *Biopolymers* **17** : 2341.

24. Pullman, B. (1978) *Intermolecular Interactions : From Diatomics to Biopolymers*, John. Wiley, New York.

25. Pack, G.R., Wang, H.Y. & Rein, R. (1972) *Chem. Phys. Lett.* **17** :381.

26. Pollak, M. & Rein, R. (1967) *J Chem. Phys.* **47** : 2045.

27. Claverie, P. (1978) *Intermolecular Interactions : From Diatomics to Biopolymers,* ed., Pullman, B., John Wiley, New York, p. 69.

28. Rein, R. (1973) *Adv. Quant. Chem.* **7** : 335.

29. Langlet, J., Claverie, P., Caron, F. & Boeuve, J.C. (1981) *Int. J. Quant. Chem.* **20** : 299.

30. Rein, R., Ornstien, R.L. & MacElroy, R.D. (1978) *Proc. Indian Acad. Sci.* **B87** : 135.

31. Ornstein, R.L. & Rein, R. (1979) *Biopolymers* **18** : 2821.

32. Sanyal, N.K., Roychoudhury, M. & Tiwari, S.N. (1985) *J. Biosci.* **8** : 713.

33. Sanyal, N.K., Tiwari, S.N., Roychoudhury, M. & Ojha, R.P. (1985) *Interface of Physical and Biological Sciences,* ed., Srivastava, S.L., Natl. Acad. Sci., India, p. 118.

34. Sanyal, N.K., Ojha, R.P., Roychoudhury, M. & Tiwari, S.N. (1986) *J. Computat. Chem.* **7** : 30.

35. Sanyal, N.K., Tiwari, S.N., Ojha, R.P. & Roychoudhury, M. (1986) *Proc. Natl. Acad. Sci., India* **A56** : 175.

36. Sanyal, N.K., Roychoudhury, M., Ruhela, K.R. & Tiwari, S.N. (1987) *J. Computat. Chem.* **8** : 604.

37. Rein, R. (1978) *Intermolecular Interactions : From Diatomics to Biopolymers,.* ed., Pullman, B., John Wiley, New York, p. 307.

38. Kitaigorodskii, A.I. (1961) *Tetrahedron* **14** : 230.

39. Kitaigorodskii, A.I. & Mirskaya, K.V. (1964) *Kristallografia* **9** : 174.

40. Caillet, J. & Claverie, P. (1975) *Acta Cryst.* **A31** : 448.

41. Caillet, J., Claverie, P. & Pullman, B. (1976) *Acta Cryst.* **B32** : 2740.

42. Bryan, R.F. (1967) *J. Chem. Soc.* 1311.

43. Pople, J.A. & Beveridge, D.L. (1970) *Approximate Molecular Orbital Theory,* McGraw Hill Book Co., New York.

44. Mishra, R.K. & Tyagi, R.S. (1973) *Liquid Crystals and Ordered Fluids,* Vol. 2, eds., Johnson, J.F. and Porter, R.S., Plenum Press, New York, p. 759.

45. Baran, W.J. & Les, A. (1979) *Mol. Cryst. Liq. Cryst.* **54** : 273.

Dielectric study of pyridine-alcohol binary liquids at 25°C

AJAY CHAUDHARI[a], SUNIL AHIRE[a], MILIND LOKHANDE[a] and SURESH MEHROTRA[b]

[a]Department of Physics, Dr. B.A.M. University, Aurangabad-431 004, India.

[b]Department of Electronics and Computer Science, Dr. B.A.M. University, Aurangabad-431 004, India.

Abstract

Dielectric relaxation study of pyridine-alcohol viz. methanol, ethanol, propan-1-ol and butan-1-ol mixtures have been carried out for 11 different concentrations at 25°C. Time Domain Reflectometry (TDR) in reflection mode has been used to measure reflection coefficient in frequency range of 10 MHz to 10 GHz. The bilinear calibration method has been used to obtain dielectric parameters viz. static dielectric constant and relaxation time. The concept of effective volume is introduced and the values of effective volume occupied by the pyridine in presence of alcohols are determined by using four models, based on the excess permittivity, excess relaxation time, the Bruggeman equation and the Kirkwood equation. The values of a parameter a which represents change in volume of constituent 1 due to constituent 2, in the mixture of constituents 1 and 2, are also determined using different models. The volume shrinks for pyridine in presence of methanol and ethanol, whereas this expands in presence of butan-1-ol and propan-1-ol.

(Keywords : time domain reflectometry/dielectric parameters/alcohols/pyridine)

Introduction

The dielectric relaxation study of solute-solvent mixtures at microwave range gives information about the molecular polarization in the system. This is related to formation of multimers in dipoles and their rotations.

The present paper reports the dielectric study related to pyridine and alcohol mixtures. Methanol, Ethanol, Propan-1-ol and Butan-1-ol are used as alcohols. The study was done at 25°C. The Time Domain Reflectometry in reflection mode has been used for the study[1-5].

Materials and Method

Pyridine (LR grade), Methanol, Ethanol (Spectroscopic grade), Propan-1-ol and Butan-1-ol (AR grade) were obtained commercially and used without further purification.

The solution were prepared at different volume percentage of pyridine (ϕ_1) in alcohols in step of 10%, at 25°C.

Apparatus used in this study was the Tektronix 7854 sampling oscillascope with 7S12 TDR unit. In this apparatus, a fast rising step voltage pulse of 200 mV amplitude and 25 ps rise time with repetition frequency of 1 kHz is generated by a tunnel diode and is propagated through a coaxial transmission line. The sample is placed at the end of the coaxial transmission line in a Standard Military Application (SMA) coaxial cell. The SMA cell used for this work had 3.5 mm outer diameter and 1.35 mm effective pin length. The step pulse generated by tunnel diode and the pulse which is reflected from the sample cell were sampled by sampling oscilloscope in the time window of 5 ns. The reflected pulse without sample $R_1(t)$ and with sample $R_x(t)$ were digitised into 1024 points in the oscilloscope memory and then transferred to PC/XT through GPIB.

A typical example of the reflected pulses without sample and with sample is shown in Fig. 1.

The temperature controller system with water bath and a thermostat has been used to maintain the constant temperature within the accuracy limit of ±1°C. The sample cell is surrounded by a heat insulating container through which the water of constant temperature using a temperature controller system is circulated. The temperature at the cell is checked using the electronic thermometer.

Data Analysis

The time dependent data were processed to obtain complex reflection coefficient spectra $\rho*(\omega)$ over the frequency range from 10 MHz to 10 GHz using Fourier transformation[6,7] as

$$\rho* (\omega) = (c/\omega d)\ [p\ (\omega)/q\ (\omega)] \tag{1}$$

where $p(\omega)$ and $q(\omega)$ are Fourier transforms of $(R_1(t) - R_x(t))$ and $(R_1(t) + R_x(t))$ respectively, c is the velocity of light, ω is angular frequency, d is effective pin length.

The complex permittivity spectra $\varepsilon*(\omega)$ were obtained from reflection coefficient spectra $\rho*(\omega)$ by using bilinear calibration method[8]. Alcohols and pyridine are chosen to be us calibrating liquids.

The experimental values of $\varepsilon*$ are fitted with the Debye expression[9-11]
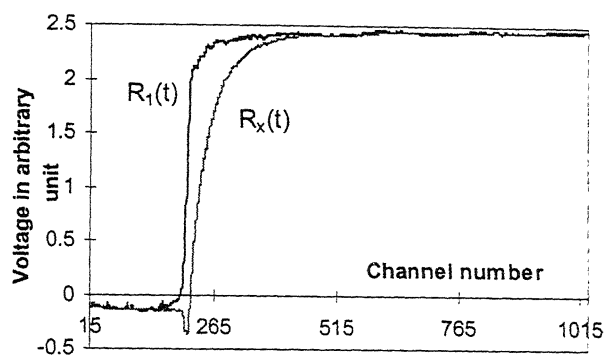
Fig. 1
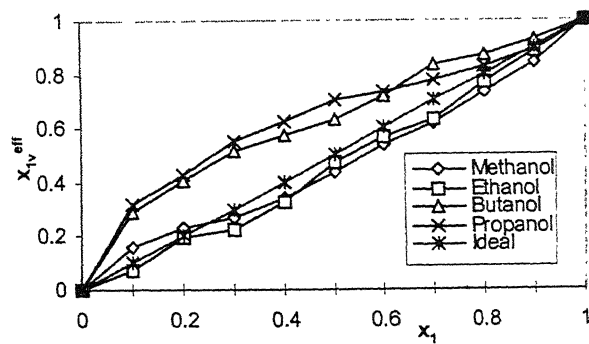
Fig. 2
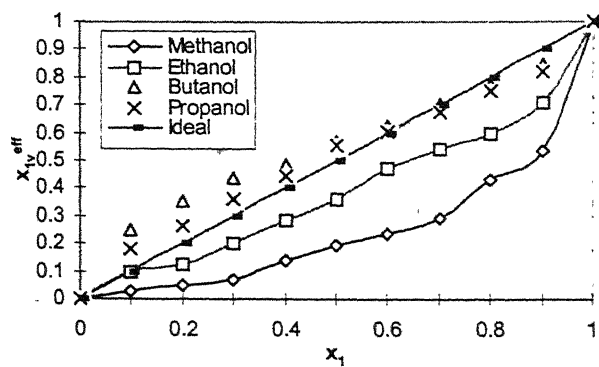
Fig. 3

$$\varepsilon^*(\omega) = \varepsilon_\infty + \frac{\varepsilon_m - \varepsilon_{\infty m}}{1 + j\omega\tau_m} \tag{2}$$

with ε_m and τ_m as fitting parameters. A non-linear least-squares fit method[12] was used to determine the values of dielectric parameters.

The value of $\varepsilon_{\infty m}$ is taken to be fixed and computed as

$$\varepsilon_{\infty m} = x_1 \varepsilon_{\infty 1} + (1 - x_1) \varepsilon_{\infty 2}$$

where $\varepsilon_{\infty 1}$ and $\varepsilon_{\infty 2}$ are permittivities at infinite frequencies for constituents 1 and 2, respectively, and x_1 is the volume fraction of the constituent 1 in the mixture. They are estimated to be as 3.5 and 4, respectively.

Results and Discussion

The density and ε_m values of pure liquids along with corresponding literature values are given in Table 1, which shows a good agreement. The static dielectric constant and relaxation time obtained by the least squares fit method are listed in Tables (2 and 3).

The solute-solvent interaction can be understood by considering non-linear effect in the values of dielectric parameters in the mixtures. The recent studies[13,14] have shown that the static dielectric constant (polarization) of associated liquids depend linearly on volume fraction. On the other hand, mixtures of associated liquids have shown relaxation times always larger than average of the individual rate of the pure components. The conventional approach in the case of ideal solutions of associated liquids with no significant structural changes with respect to pure components is that a linear behaviour of the logarithm of the relaxation rate should be obtained i.e.

$$\ln(\tau(x_{1m})) = x_{1m} \ln(\tau_1) + (1 - x_{1m}) \ln(\tau_2) \tag{3}$$

where x_{1m} is mole fraction of the component 1. m, 1 and 2 represent mixture, component 1 and 2 respectively. The suffixes 1 and 2 represent pyridine and alcohols, respectively, in the present paper.

It is useful to define the effective volume fraction as follows :

$$x_{1v}^{eff} = \frac{\varepsilon_m(x_1) - \varepsilon_m(0)}{\varepsilon_m(1) - \varepsilon_m(0)} \qquad (4)$$

and the effective mole fraction as

$$x_{1m}^{eff} = \frac{\ln(\tau_m(x_1)) - \ln(\tau_m(0))}{\ln(\tau_m(1)) - \ln(\tau_m(0))} \qquad (5)$$

where $\varepsilon_m(x_1)$ is the dielectric constant of mixture with the volume concentration of component 1 as x_1 in the mixture 1.

The value of the x_{1v}^{eff} may be calculated from x_{1m}^{eff} as follows :

$$x_{1v}^{eff} = \frac{x_{1m}^{eff}}{x_{1m}^{eff} + \left(1 - x_{1m}^{eff}\right)/f} \qquad (6)$$

where $f = (\rho_2 M_1 / \rho_1 M_2)$; ρ_i and M_i represent density and molecular weight respectively, for constituent i ($i = 1, 2$) .

Table 1 – Comparison of data for the pure liquids used with the literature values at 25°C.

Liquid	ε_0		$\rho/gm.cm^{-3}$	
	This work	Lit.	This work	Lit.
Methanol	32.05	32.63	0.78695	0.78698
Ethanol	24.08	24.30	0.78509	0.78506
Propan-1-01	20.21	20.10	0.78124	0.7812
Butan-1-01	17.22	17.10	0.80596	0.8059
Pyridine	12.02	12.30	0.98113	0.9811

The plots of x_{1v}^{eff} vs x_1 are given in Fig. (2 and 3). The ideal behaviour is shown by the straight line. The effective values are less than the ideal behaviour for smaller alcohols. As size of the alcohol molecule increases, the effective volume increases. This indicates that there is a tendency to occupy more volume by pyridine molecules in presence of larger alcohols whereas it occupies smaller volume in presence of alcohol with smaller size. This

Table 2 – Static dielectric parameters (ε_m) for pyridine-alcohol system at 25°C.

x_2	Methanol	Ethanol	Propan-1-ol	Butan-1-ol
0.0	32.05(11)	24.08(5)	20.21(1)	17.22(2)
0.1	28.87(14)	23.17(10)	17.22(8)	15.73(11)
0.2	27.45(8)	21.73(4)	16.72(16)	15.12(10)
0.3	26.63(5)	21.39(4)	15.68(10)	14.53(5)
0.4	25.27(7)	20.11(4)	15.11(5)	14.23(3)
0.5	23.33	18.36(3)	14.45(1)	13.93(8)
0.6	21.31(9)	17.26(3)	14.21(4)	13.49(3)
0.7	19.78(5)	16.52(4)	13.86(15)	12.89(4)
0.8	17.41(9)	14.84(2)	13.46(21)	12.71(4)
0.9	15.14(5)	13.44(4)	12.92(21)	12.38(2)
1.0	12.02(2)	12.02(2)	12.02(2)	12.02(2)

means that the volume occupied by pyridine exerts larger effective repulsive forces to volume occupied by the alcohols, as the size of the alcohol increases.

In the paper[4], the Bruggeman formula was modified to explain the behaviour of the experimental data related to binary polar liquids as follows :

$$f_B = \left(\frac{\varepsilon_m(x_1) - \varepsilon_m(1)}{\varepsilon_m(2) - \varepsilon_m(1)} \right) \left(\frac{\varepsilon_m(2)}{\varepsilon_m(1)} \right)^{1/3} = \left(1 - x_{1v}^{eff} \right) \tag{7}$$

where $\qquad x_{1v}^{eff} = [a - (a-1)x_1]x_1$

$$\tag{8}$$

The above equation satisfies the boundary conditions at $x_1 = 0$ and $x_1 = 1$. The value of $a = 1$ corresponds to no interaction between constituent 1 and 2, $a < 1$ corresponds to reduction of the effective volume occupied by the constituent 1 due to constituent 2, and $a > 1$ corresponds to increase in the effective volume of the constituent 1, due to the constituent 2.

Table 3 – Relaxation time (τ_m) for pyridine-alcohol system at 25°C.

x_1	Methanol	Ethanol	Propan-1-ol	Butan-1-ol
0 0	52.37	145.84(80)	278 86(11)	512.04(17)
0.1	48.07(45)	102.46(10)	148.43(14)	212.35(52)
0.2	44.82(27)	94.28(43)	110.42(18)	141.72(31)
0.3	42.36(17)	73.18(31)	78.90(11)	103.98(10)
0.4	34.87(25)	56.54(19)	59.82(82)	85.13(21)
0.5	30.63(3)	45.37(39)	41.12(4)	61.60(13)
0.6	28.20(32)	33.62(21)	35.77(25)	49.42(33)
0.7	25.02(24)	27.77(19)	28 43(91)	36.76(38)
0.8	19.45(32)	24.22(15)	22.17(47)	27.21(36)
0.9	16.75(24)	18.82(82)	17.75(32)	19.49(28)
1.0	10.11(29)	10.11(29)	10.11(29)	10.11(29)

Table 4 – Values of a for pyridine-alcohol systems.

'a'	Methanol	Ethanol	Propan-1-01	Butan-1-ol
$a_{\varepsilon 0}$	0.770	0.780	1.719	1.791
a_τ	– 0.450	0.371	1.309	1.107
a_B	0.494	0.582	1.606	1.626
a_K	0.901	0.914	1.652	1.756

The Kirkwood correlation factor g[15] is also a parameter for getting structural information. In the mixture, the effective volume x_{1v}^{eff} can be obtained by using the following Kirkwood equation for mixtures,

$$\frac{4\Pi N}{9kT}\left(\frac{\mu_1^2 \rho_1 g_1}{M_1} x_{1v}^{eff} + \frac{\mu_2^2 \rho_2 g_2}{M_2}\left(1 - x_{1v}^{eff}\right)\right) = \frac{(\varepsilon_m - \varepsilon_{\infty m})\ (2\varepsilon_m + \varepsilon_{\infty m})}{\varepsilon_m\ (\varepsilon_{\infty m} + 2)^2} \qquad (9)$$

where μ_i $(i = 1, 2)$ are dipole moments of constituents 1, 2; g_i $(i = 1, 2)$ are correlation factors of constituents 1, 2; k is the Boltzmann factor and T is temperature of the mixture.

The correlation factors of pure liquids 1 and 2 are computed by using the Kirkwood equation for pure liquids. By using Eqn. (8) and (9), it is possible to determine the corresponding values of a.

$a_{\varepsilon 0}$, a_τ, a_B and a_k are values of a as determined by values of x_{1v}^{eff} from Eqn. (4), (5), (7) and (9), respectively, and using Eqn. (6) and (8). These values are listed in Table 6. It is interesting to observe that as size of alcohol increases, the value of a also increases. This indicates that the effective volume of pyridine gets increased due to the larger size of the alcohols.

The values of a obtained from the relaxation data are much smaller than corresponding values of a obtained from polarization volume. This is expected, as relaxation time involves dynamical behaviour of polarization, so more sensitive to long range intermolecular interactions.

Conclusion

The Onsager dielectric of pure liquids assumes a cavity inside the liquid. The radius of the cavity is computed by using the density. We have computed the values of effective volumes in the mixture by using four different models based on the excess permittivity, excess logarithmic of relaxation time, the modified Bruggemann equation and the Kirkwood equation, respectively. The parameter a which represents significance of change in volume, is determined. This provides a unified approach to understand the interaction between two constituents in the liquid mixtures, using different models.

Acknowledgement

References

1. Kumbharkhane, A.C., Helambe, S.N. & Mehrotra, S.C. (1993) *J. Chem. Phys.* **23** : 2205.

2. Puranik, S.M., Kumbharkhane, A.C. & Mehrotra, S.C (1992) *J. Chem. Soc. Faraday Trans.* **88** : 433.

3. Puranik, S.M., Kumbharkhane, A.C. & Mehrotra, S.C (1991) *J. Chem. Soc. Faraday Trans.* **87** : 1569.

4   Kumbharkhane, A.C., Puranik, S.M. & Mehrotra, S.C. (1991) *J. Sol. Chem.* **20** : 12.

5. Puranik, S.M., Kumbharkhane, A.C. & Mehrotra, S.C. (1991) *J. Micro. Pow. EM energy* 26 : 196.

6. Shannon C.E. (1949) *Proc. IRE* 37 : 10.

7   Samulon, H.A. (1951) *Proc. IRE* 39 : 175

8. Cole, R H , Berbarian, J G., Mashimmo, S., Chryssikos, G., Burns, A. & Tombari E. (1989) *J. Appl. Phys* 66 : 793.

9. Havrilliak, S. & Negami, S. (1996) *J. Polym. Sci. Polym. Symp.* 99.

10 Cole, K S. & Cole, R.H (1941) *J. Chem. Phys.* 9 : 341.

11 Davidson, D.W. & Cole, R.H. (1950) *J. Chem. Phys.* 18 : 1484

12 Bevington, P.R. (1969) *Data reduction and error analysis for the physical sciences*, McGraw Hill, New York.

13 Mashimo, S., Umehara, T. & Redlin, H. (1991) *J. Chem. Phys.* 95 : 6275.

14. Bao, J., Swicord, M.L & Davies, C.C. (1995) *J. Chem. Phys.* 104 : 4441

15. Frohlich, H. (1949) *Theory of Dielectrics*, Oxford University Press, London.